Assessment of Global Wetlands Using a Conceptual Framework of Entropy and Climate Extremes

M.Tech. Thesis

By

NAKKA NAVEEN KUMAR

(2302104015)

DEPARTMENT OF CIVIL ENGINEERING

INDIAN INSTITUTE OF TECHNOLOGY INDORE

MAY 2025

Assessment of Global Wetlands Using a Conceptual Framework of Entropy and Climate Extremes

A THESIS

Submitted in partial fulfillment of the requirements for the award of the degree of

Master of Technology

In

Water, Climate, and Sustainability

by

NAKKA NAVEEN KUMAR
(2302104015)

DEPARTMENT OF CIVIL ENGINEERING
INDIAN INSTITUTE OF TECHNOLOGY INDORE
MAY 2025

INDIAN INSTITUTE OF TECHNOLOGY INDORE

CANDIDATE'S DECLARATION

I hereby certify that the work which is being presented in the thesis entitled **Assessment of Global Wetlands Using a Conceptual Framework of Entropy and Climate Extremes,** in the partial fulfilment of the requirements for the award of the degree of **Master of Technology** in **Water, Climate, and Sustainability** and submitted in the **Department of Civil Engineering**, **Indian Institute of Technology Indore**, is an authentic record of my work carried out during the period from **July 2023** to **May 2025**. Under the supervision of Prof. Manish Kumar Goyal, Department of Civil Engineering, Indian Institute of Technology Indore.

The matter presented in this thesis has not been submitted by me for the award of any other degree of this or any other institute.

N. Naveen Kumar 29/05/2025

Signature of the student with date
NAKKA NAVEEN KUMAR

This is to certify that the above statement made by the candidate is correct to the best of my/our knowledge.

Manish

Signature of the Supervisor of
M.Tech. Thesis dated 2nd June 2025
(Prof. Manish Kumar Goyal)

NAKKA NAVEEN KUMAR has successfully given his M.Tech. Oral Examination held on **24 May 2025**.

Manish

Signature of the Supervisor of M.Tech. Thesis
Date: 2nd June 2025

Convener, DPGC
Date:

Acknowledgment

I express my profound gratitude to Prof. Manish Kumar Goyal for his exceptional mentorship, insightful guidance, and steadfast support throughout my M.Tech journey. His encouragement, constructive feedback, and the academic freedom he provided were pivotal to the successful completion of this research.

In IIT Indore, I extend my sincere thanks to Dr. Priyank J. Sharma (Asst. Prof), Dr. Mayur Shirish Jain (Asst. Prof), Dr. Ashootosh Mandpe (Asst. Prof), and Dr. Mohd. Farooq Azam (Assoc. Prof) from the Department of Civil Engineering, Dr. Unmesh Khati (Asst. Prof), Dr. Bhargav Vaidya (Assoc. Prof), and Dr. Saurab Das (Assoc. Prof) from DAASE, as well as Prof. Pritee Sharma, Dr. Mohanasundari Thangavel (Asst. Prof), and Prof. Nirmala Menon from the School of HSS, for their teaching and support during my coursework at IIT Indore. The dedication of all faculty and staff across departments has been crucial to my academic and research development.

Special gratitude goes to Dr. Shekar Singh and Mr. Deepak Mishra for their assistance with my project and to Mr. Kuldeep Singh Rautela for his help with the bubble plot. I am thankful to my seniors and lab colleagues for their cooperation and support. I also express my appreciation to my batchmates in the Water, Climate, and Sustainability program for being a source of motivation and friendship throughout my time in the M.Tech program. I am grateful to the faculty under whom I served as a teaching assistant and to my fellow TAs for their collaboration and support. I acknowledge the non-teaching staff, employees, and contractual staff for their essential services, both directly and indirectly. My sincere thanks also go to the authors and researchers whose publicly accessible data, tools, methodologies, and findings made my research possible.

Above all, I am indebted to IIT Indore for providing me with a nurturing environment, knowledge, and opportunities that have profoundly influenced my growth and will remain with me for life.

Nakka Naveen Kumar

2302104015

Abstract

Wetlands are highly sensitive ecosystems whose stability is strongly influenced by rainfall variability and extremes. While previous studies have examined wetland shrinkage and precipitation extremes separately, this study uniquely integrates entropy-based metrics, Standardized Variability Index using Apportionment Entropy (SVI_{AE}) and Marginal Entropy (SVI_{ME}), with 12 Standardized extreme precipitation indices to assess hydroclimatic risk across 2,490 Ramsar wetlands worldwide. Using high-resolution precipitation datasets and CMIP6 climate projections, we analysed historical (1951 - 2024) and future (2025 - 2100) scenarios under SSP 245 and SSP 585 pathways. Results reveal a clear rise in monthly rainfall variability (SVI_{AE}), especially under SSP 585, in areas including Africa, South Asia, and West Asia; in contrast, yearly variability (SVI_{ME}) remains stable, masking critical intra-annual instability. Extreme indices (e.g., R95pTOT, Rx5) show significant intensification under SSP 585, with more than 40% of wetlands falling into high-risk zones for unpredictability and rainfall intensity. Arid wetlands, despite low rainfall, face increasing flash-flood risks due to more intense and erratic rainfall events. These findings emphasize that increasing rainfall does not guarantee stability; rather, the combination of variability and extremes amplifies wetland vulnerability. This study provides a novel, integrated framework for identifying climate-sensitive wetlands and guiding adaptive conservation planning.

Keywords: Ramsar wetlands, Entropy, Rainfall variability, Precipitation extremes, Climate projections.

TABLE OF CONTENTS

List of Figures

List of Tables

Abbreviations and Acronyms

IPCC - Intergovernmental Panel on Climate Change

NASA - National Aeronautics and Space Administration

NEX - GDDP - NASA Earth Exchange's set of daily, downscaled climate projections

GCM - General Circulation Model

GMFD - Global Meteorological Forcing Dataset

BCSD - Bias Correction Spatial Downscaling

CMIP6 - Coupled Model Intercomparison Project Phase 6

CF - Climate Forecast

IOC - Intergovernmental Oceanographic Commission

SSP – Shared Socioeconomic Pathways

SSP 245 - Shared Socioeconomic Pathway 2 represents a moderate greenhouse gas emission scenario, anticipating an increment of 4.5 W/m² radiative forcing by 2100

SSP 585 - Shared Socioeconomic Pathway 5 marks the highest end of emission scenarios, anticipating an increment of 8.5 W/m² radiative forcing by 2100

MME - Multi-model Ensemble Mean

WMO - World Meteorological Organization

RCP - Representative Concentration Pathway

AE - Apportionment Entropy

ME - Marginal Entropy

NCCS - NASA Centre for Climate Simulation

SVI - Standardized Variability Index

SVI_{AE} - Standardized Variability Index of Apportionment entropy

SVI_{ME} - Standardized Variability Index of Marginal entropy

CLIVAR - Climate and Ocean Variability, Predictability and Change

ETCCDI - Expert Team on Climate Change Detection and Indices

JCOMM - Joint WMO-IOC Technical Commission for Oceanography and Marine Meteorology

1. Introduction

Wetlands represent some of the planet's most essential ecosystems, delivering key functions that include the preservation of biodiversity (Dertien et al., 2020), natural water treatment (Teuchies et al., 2013; Xu et al., 2024), flood regulation (Golden et al., 2021; Orimoloye et al., 2020), carbon sequestration (Jamion et al., 2023; Lolu et al., 2020; Were et al., 2019), and regulation of atmospheric conditions (Moomaw et al., 2018; Nyberg et al., 2022; Reid et al., 2005). In response to the ongoing degradation of wetlands worldwide and the resulting threats to both biodiversity (Valenti et al., 2020) and human wellness (Fluet-Chouinard et al., 2023; Kundu et al., 2024; Sharma and Naik, 2024; Sharma et al., 2021). The Ramsar Convention, instituted in 1971, serves as the principal global accord devoted exclusively to safeguarding and ensuring the long-term viability of wetlands (Geijzendorffer et al., 2019; Kingsford et al., 2021; Ramsar Convention, 1971). While the Ramsar Convention has advanced wetland conservation for over five decades (Kingsford et al., 2021). There is growing recognition that wetlands are dynamic systems, impacted not only by direct human intervention but also by a variety of natural and environmental influences (Day et al., 2024; Moi et al., 2022; Yan et al., 2022; M. Zhang et al., 2022) but also by long-term climatic shifts (Birnbaum et al., 2021; R. Wang et al., 2023; Xiong et al., 2023). Recent worldwide evaluations, such as those conducted by the IPCC (Dawson and Spannagle, 2020; IPCC, 2022, 2021; Kikstra et al., 2022; Skea et al., 2021) have emphasized the vulnerability of wetland ecosystems to a variety of interconnected threats arising from shifting climate patterns (Schuur et al., 2015; X.-L. Wang et al., 2024; Xi et al., 2021), including rising temperatures (Butterfield and Palmquist, 2023; Goyal et al., 2024; Jain et al., 2025), shifting precipitation patterns (Singh et al., 2024), an upward trend in sea surface levels (Goyal et al., 2023b; Lovelock et al., 2015; Parkinson and Wdowinski, 2022; Schuerch et al., 2018; Spencer et al., 2016), and increasingly frequent extreme climatic events (Junk et al., 2013; Moomaw et al., 2018; Singh et al., 2024). Such changes can disrupt the hydrological regimes upon which wetlands depend, altering water availability, vegetation dynamics (Afuye et al., 2024, 2022; Zheng et al., 2021), carbon flux processes, and the arrangement of species across habitats (Aguirre-Liguori et al., 2021; Liu et al., 2022; Seneviratne et al., 2012).

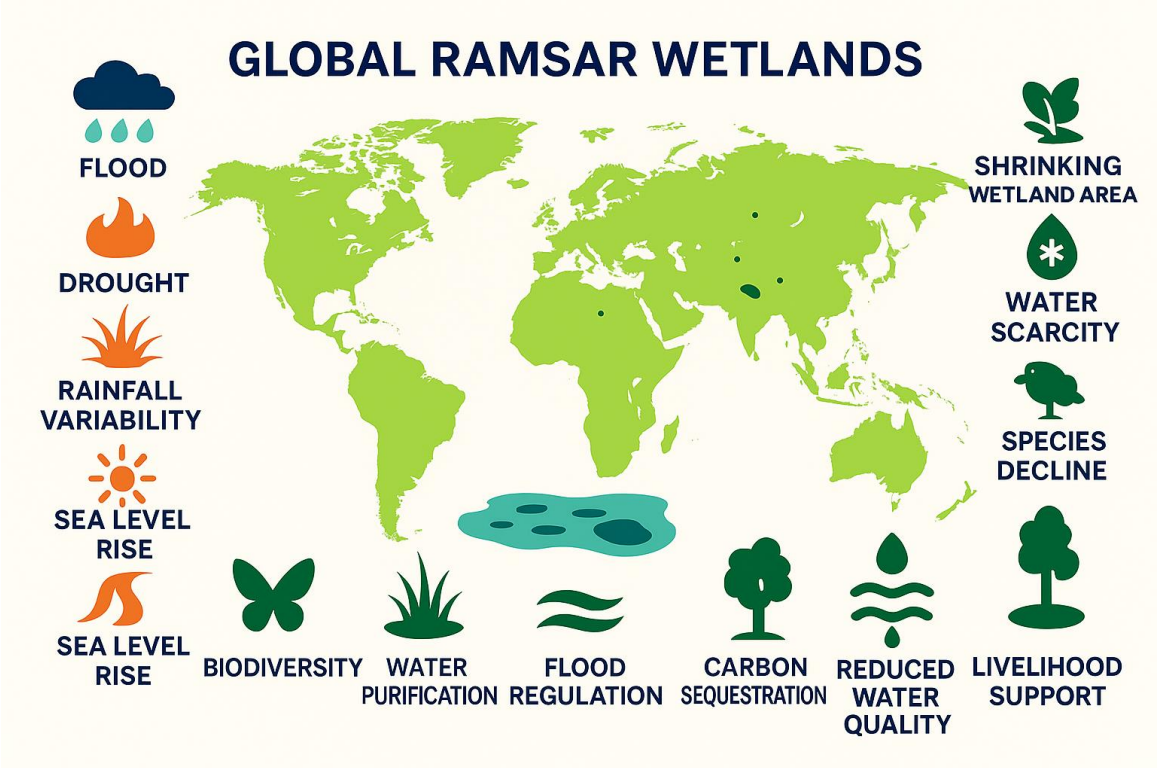

Figure 1: Schematic representation of global Ramsar sites, major climate change threats, associated impacts on wetland health and biodiversity, and the critical benefits delivered by these ecosystems

Among the key issues confronting wetland science is understanding how climate change alters rainfall behavior in ways that threaten wetland function and resilience (Erwin, 2009; Grieger et al., 2020; Sandi et al., 2020)**,** as shown in Figure 1. Conventional hydrological analyses typically focus on average precipitation changes or general rainfall trends (AlSubih et al., 2021; Bayazit, 2015). However, such approaches may overlook crucial aspects of variability, such as the distribution and predictability of rainfall events across time (Singh and Kumar, 2024; Yaduvanshi et al., 2019; Yeşilırmak and Atatanır, 2016; Zhang et al., 2021). Given the challenges of modeling nonlinear hydrological systems, entropy methods offer a principled way to assess rainfall's spatiotemporal complexity (Feng et al., 2013; Mishra et al., 2009; Pang et al., 2023; Singh, 2011). Rooted in information theory (Bandt and Pompe, 2002; Brunsell, 2010; Shannon, 1948; Shuangcheng et al., 2006; L. Zhang et al., 2019). Entropy quantifies the degree of disorder or uncertainty in a system (Sreeparvathy and Srinivas, 2022; C. Zhang et al., 2019). In hydrology, entropy has been adapted into several metrics, including marginal entropy, apportionment entropy (Chetan Kumar et al., 2024; Heshu Li et al., 2021), and measuring the unpredictability and complexity of rainfall regimes across diverse temporal and spatial dimensions through

intensity entropy analysis **(**Alemayehu et al., 2020; Krstanovic and Singh, 1992; Lu et al., 2022; Maruyama et al., 2005; Roushangar et al., 2019; Singh et al., 2022; Singh, 2011, 1997).

Marginal entropy reflects the uncertainty in the magnitudes of rainfall (Bayat et al., 2021), whereas apportionment entropy captures how rainfall is distributed across a defined period (e.g., monthly or annually) (Sarkar and Maity, 2021; H. Wang et al., 2024). Higher entropy indicates less predictability and potentially greater hydroclimatic stress for ecosystems dependent on stable water inputs (Sarkar and Maity, 2022). The development of Standardized Variability Indices (SVIs), such as SVI_{ME} (based on marginal entropy) and SVI_{AE} (based on apportionment entropy), enables the standardized assessment of rainfall variability across regions and scales (Guntu and Agarwal, 2020; Rolim et al., 2022). These indices provide a framework for comparing entropy-derived variability at different wetland locations, highlighting areas where climate change may be amplifying unpredictability in precipitation inputs (Guntu et al., 2020b; Kawachi et al., 2001). Recognizing such patterns plays a vital role in the stewardship of wetlands, as areas with pronounced rainfall variability are at heightened risk of drying out, flooding, or experiencing shifts in ecological balance (Bastos et al., 2023; Palmer et al., 2023; Wu et al., 2024).

Beyond heightened variability, the occurrence and magnitude of extreme precipitation events are also escalating (de Vries et al., 2024; Gupta et al., 2023; Myhre et al., 2019) and have emerged as key climate risks (Swain et al., 2022) for wetlands (Goyal et al., 2022). Extreme rainfall can result in flooding (Baig et al., 2022; Kumar et al., 2023), erosion, habitat disruption (Kaboli et al., 2021), and shifts in wetland hydrology (Goyette et al., 2023; Granata and Di Nunno, 2025), especially in systems with limited buffering capacity (Åhlén et al., 2022). To evaluate such changes, ETCCDI has put together a collection of carefully defined indices. Each created to consistently measure severe precipitation instances, such as R10 (yearly tally of days during which rainfall reaches or surpasses 10 millimeters, reflecting the presence of high-intensity precipitation occurrences), PRCPTOT (total yearly precipitation accumulated exclusively on days classified as wet, meaning those with rainfall amounts of 1 millimeter or more) (Gehlot et al., 2021; Maharjan et al., 2023; L. Wang et al., 2023; Zou et al., 2021), R95pTOT (very wet days) (Goffin et al., 2024; Qin et al., 2023; Sebaziga et al., 2025; Yu et al., 2020), and RX1day (maximum 1-day rainfall) (Regueira and Wanderley, 2022; Tung et al., 2022; Zittis et al., 2021). Employing such

standardized indices allows for coherent evaluation of extreme precipitation trends in wetland hydrology, especially where buffering capacity is limited (Ogolo and Matthew, 2022).

Numerous studies have applied ETCCDI indices to assess regional and global changes in extreme rainfall (Chervenkov and Slavov, 2021; Yin and Sun, 2018). For instance, increased precipitation risks have been documented in the permafrost zones of Siberia (Hjort et al., 2022; Melnikov et al., 2024; Nitzbon et al., 2020; Wang et al., 2021), deltas prone to frequent inundation the lower Asian peninsula and Southeast Asian mainland (Becker et al., 2024; Chan et al., 2024; Rakkasagi and Goyal, 2025; Skliris et al., 2022), and Central Asian Arid and semi-desert areas (Hu et al., 2019; Yao et al., 2021; M. Zhang et al., 2022). Earlier analyses using CMIP5 (Sillmann et al., 2013) and CMIP6 models (Dong and Dong, 2021; Kim et al., 2020; Wehner et al., 2021) have consistently demonstrated increased magnitude and frequency of intense precipitation occurrences under both mid-range and high-end emission trajectories (Almazroui et al., 2021; Deepa et al., 2024; Goyal et al., 2023a; Kuinkel et al., 2024), although with regional variability and uncertainty (Singh et al., 2024). Ramsar sites, many of which are located in hydrologically sensitive zones, are particularly vulnerable to these extremes (Baker et al., 2021; Popoff et al., 2021; Y. Zhang et al., 2022). Even a small increase in rainfall intensity or duration can overwhelm the hydrological balance, threatening ecosystem stability and human livelihoods dependent on wetland services (Hempattarasuwan et al., 2021; Hussain et al., 2024; Imdad et al., 2025; Seneviratne et al., 2012; Shukla et al., 2021).

While considerable research has focused separately on rainfall variability (using entropy) (Balzter et al., 2015; Choobeh et al., 2024; Krstanovic and Singh, 1992; Mishra et al., 2009) and rainfall extremes (Alexander et al., 2009; Dittus et al., 2018; Lagos et al., 2008; Lemus-Canovas, 2022; Singh et al., 2023; Yin et al., 2023) (using ETCCDI indices), few studies have attempted to integrate these two dimensions. Yet, understanding both the “shape” and “size” of rainfall variability is crucial for holistic wetland risk assessment. Entropy-based metrics offer insights into regular or irregular rainfall patterns (Du et al., 2022; Ghorbani et al., 2021; Keum and Coulibaly, 2017; Tatli and Dalfes, 2021). , while extreme indices quantify the magnitude and frequency of impactful events (Duchenne-Moutien and Neetoo, 2021; Liaqat et al., 2024; McDowell et al., 2023; Ndehedehe, 2023; Peters-Lidard et al., 2021). For instance, a wetland may receive the same annual precipitation across two

periods. Still, one may involve frequent moderate rains (low entropy, low extremes), while the other includes long dry spells interrupted by intense storms (high entropy, high extremes). These differences can have profound ecological consequences.

2. Comprehensive Literature Analysis

Recent research efforts have been directed toward exploring how Ramsar wetlands and related hydrological systems are responding to climate change, land use shifts, and increasing hydroclimatic extremes. Recent studies have combined long-term observations, advanced modeling, and innovative analytical tools, such as entropy-based metrics, to unravel the complex patterns of wetland vulnerability, rainfall variability, and the risks posed by extreme weather events. This section reviews key research contributions that collectively advance our knowledge of wetland dynamics under changing environmental conditions.

Singh et al. (2024) conducted a climate vulnerability assessment of Indian Ramsar wetlands by analyzing historical inundation data and employing machine learning to predict future patterns. Their findings revealed that some sites, including the Udhayamarthandapuram Bird Sanctuary, are experiencing declining inundation, highlighting their susceptibility to shifts in climate, together with hazardous weather phenomena. Anand et al. (2024) examined how shifts in climate and land use together affect the hydrological characteristics of the Loktak Lake catchment. Their projections indicate that both temperature and precipitation are projected to increase during the middle and latter parts of the century, resulting in increased streamflow and water yield. These results underscore the importance of integrated watershed management in fragile wetland environments. The significance of floodplain representation in hydrological models was examined by Schrapffer et al. (2020), who used the ORCHIDEE model to simulate the Pantanal's water cycle. Their study found that increased evapotranspiration from floodplains can alter local temperature and humidity gradients, demonstrating the crucial role of floodplain processes in regional climate regulation.

Hongwei Li et al. (2021) addressed the escalating threat of drought in drylands. Climate models suggest that the global average length of droughts may increase by approximately twofold by 2100, particularly under high greenhouse gas pathways like SSP 585. Such prolonged dry spells are anticipated to heighten vulnerabilities in agricultural systems, freshwater availability, and ecological resilience, with arid and semi-arid zones facing the most severe consequences.

Hardouin et al. (2024) utilized soil moisture projections and the TOPMODEL framework to assess future changes in wetland extent globally. Their results suggest that wetlands are likely to contract in regions such as the Mediterranean and western Amazon, while some expansion may occur in Central Africa, excluding the Congo Basin. Alaminie et al. (2023) emphasized the significance of accurate hydrological modeling to improve flood forecasting in Ethiopia's Lake Tana basin. Employing the Wflow_sbm model alongside CMIP6 climate projections, their research indicates that the region is likely to experience a greater number and intensity of heavy rainfall episodes, thereby elevating the threat of flooding in the area.

The integration of wetlands with reservoir operations as a means aimed at lowering vulnerability to floods and water scarcity was investigated by Wu et al. (2023). Their findings indicate that while this approach can help mitigate hazards, it is insufficient to fully address the hazards posed by climate change, pointing to the need for additional adaptive approaches. Xu et al., (2024) evaluated how climate change affects various systems in North American inland wetlands, projecting significant reductions in wetland area and disruptions to seasonal inundation patterns. These changes threaten biodiversity in regions like the upper Mississippi, Southeast Canada, and the Everglades. In Tanzania, Mollel et al., (2023) modeled the impact of climate shifts on water resources in the Usangu catchment by integrating the SWAT model with outputs from an ensemble of GCMs. Their projections for 2030 - 2060 indicate increases in precipitation and temperature, but also suggest that evapotranspiration will rise while water yield and groundwater recharge decline, particularly during wetter periods.

Rakkasagi et al., (2024) evaluated projected threats from intense precipitation events to India's coastal Ramsar wetlands, using fuzzy logic and return period analysis. The study identified high-risk zones and emphasized the role of urbanization and sedimentation in exacerbating flood vulnerability. Entropy-based approaches have provided new insights into rainfall variability. Hassanlu et al., (2023) applied the Concentration Index and Shannon's Entropy to daily rainfall data across Iran, revealing that southern regions face high rainfall concentration and variability, increasing both drought and flood risks, while the northwest benefits from more stable rainfall patterns. Wu et al., (2022) simulated future conditions regarding hydrometeorological events and assessed the role of wetlands in mitigating floods within the Nenjiang River basin in Northeast China. Their results indicate

that wetlands are effective at lessening the length and severity of minor flood events. Still, their capacity to buffer against flooding declines when faced with more severe events driven by increasing precipitation extremes.

Chapagain et al., (2021) projected future episodes of extreme weather and evaluated their influence on key sectors in the Karnali Basin, Nepal. The study suggests that the region will experience pronounced warming, more intense rainfall, and a heightened incidence of severe weather, imposing notable burdens on sectors that are especially susceptible to climate impacts. Abraham and Kundapura (2022) examined multi-decade variations in rainfall and thermal conditions within three humid tropical catchments in Kerala, India. Their results indicate declining annual and seasonal rainfall, rising extreme rainfall events, and increasing temperatures, all of which contribute to greater climate variability, water stress, and flood risk, emphasizing the need for proactive adaptation.

Together, these studies provide a comprehensive view of the challenges and dynamics shaping Ramsar wetlands and similar ecosystems, highlighting the importance of advanced modeling, entropy-based analysis, and integrated management strategies amid rapidly intensifying climate shifts. The incorporation of entropy analysis alongside measures of precipitation extremes enables a more refined and complete assessment of climate-driven pressures affecting wetlands. When high levels of entropy coincide with frequent extreme precipitation events, this combination may signal fundamental instability in wetland hydrology, highlighting areas where urgent adaptation and management interventions are required. In contrast, Wetlands with lower entropy levels (indicating stable hydrological patterns) and fewer extreme hydrological events demonstrate greater resilience to shifts in water regimes, such as droughts, floods, or altered precipitation dynamics. Mapping those patterns across global Ramsar sites enables the identification of priority areas for conservation, informs the strategic allocation of resources, and supports the development of early warning systems for wetland vulnerability.

To address the critical gap in understanding how both rainfall variability and extremes impact wetlands, this study systematically examines these factors across 2,490 Ramsar wetland sites worldwide. Leveraging high-resolution gridded precipitation datasets and projections from the CMIP6 climate model ensemble, we calculate entropy-based indices, specifically the Spatiotemporal Variability Index for Marginal Entropy (SVI_{ME}) and Apportionment Entropy (SVI_{AE}), alongside 12 standardized extreme precipitation indices.

Analyses encompass both the baseline period (1951 - 2024) and future projections (2025 - 2100) for the middle and extreme emission trajectories. This dual-framework approach allows for the identification of wetland sites that are not only experiencing more frequent or intense rainfall extremes but are also becoming increasingly unpredictable in their hydrological regimes.

The specific objectives of this research are to:

1. Evaluate rainfall variability at monthly and annual timescales for all Ramsar wetlands using entropy-based indices (SVI_{ME} and SVI_{AE}).
2. Analyse historical and projected trends in 12 ETCCDI-based metrics for quantifying intense precipitation occurrences using multi-model CMIP6 ensembles under scenarios reflecting medium and severe climate forcing.
3. Identify global and regional hotspots where high entropy coincides with increasing precipitation extremes, indicating zones of heightened vulnerability.
4. Provide a multi-dimensional risk assessment framework to support adaptive wetland management and inform policy decisions at national and international levels.

By bridging the gap between statistical measures of variability and the real-world impacts of hydrological extremes, this study advances a more holistic understanding of climate change risks facing wetland ecosystems. The integration of entropy metrics with indices of extreme precipitation offers a powerful approach for detecting subtle but significant shifts in hydroclimatic behavior, thereby helping to protect and responsibly oversee some of the planet’s most ecologically significant and sensitive regions.

3. Study Area

This study undertakes a thorough worldwide evaluation of Ramsar wetlands designated for their international importance under the Convention of Ramsar, a multilateral agreement from 1971 designed to encourage the preservation and responsible utilization of wetland habitats. As of the study period, there are 2,536 designated Ramsar sites worldwide, spanning a total area of approximately 25,79,89,130 hectares. From this global dataset, our study includes 2,490 sites with complete geospatial and attribute information suitable for climatic and ecological analysis.

Ramsar wetlands, distributed across all inhabited continents, are ecologically diverse and serve as critical ecosystems for biodiversity, water regulation, carbon storage, and livelihoods. Due to their sensitivity to hydrological changes, such ecosystems are highly susceptible to climate-related impacts, including irregular precipitation, pronounced temperature variability, and species composition or range (Junk et al., 2013; Finlayson et al., 2006). It makes them not only conservation priorities but also key natural laboratories for understanding climate-driven ecological transitions. Thus, their inclusion in global climate change assessments is indispensable.

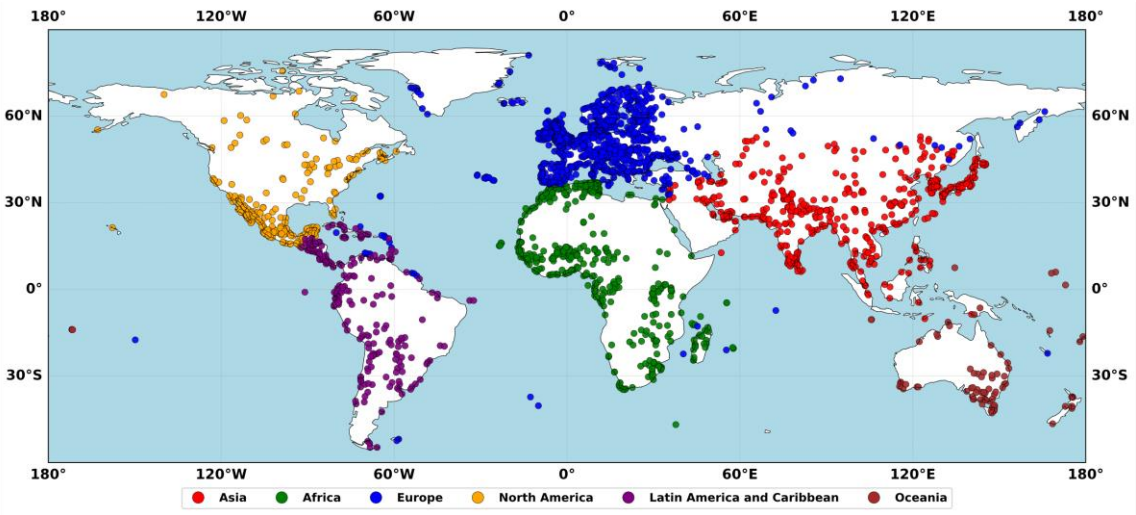

Figure 2: Global distribution of Ramsar sites categorised by continent.

Each dot in the figure corresponds to a specific Ramsar wetland, with colors indicating their broad geographic regions as defined by the Ramsar Sites Information Service. The analysis includes nearly all designated sites from each region, specifically: 424 of 431 from the African continent, 439 of 445 from Asia, 1,121 of 1,134 from Europe, 212 of 218 from

the Latin American and Caribbean region, 213 of 222 from North America, and 81 of 86 from Oceania (see Figure 2). This extensive spatial distribution ensures a near-complete global sample, allowing robust cross-regional comparisons of climatic trends and site-specific responses of wetlands from 172 countries (Davidson, 2014; Ramsar Convention, 1971; Ramsar Convention Secretariat et al., 2018), enabling broad-scale spatial analysis and robust intercontinental comparison. India, which became a contracting party in 1982, presently has 89 designated Ramsar sites covering about 1.36 million hectares, the largest number among Southeast Asian nations. These sites span a wide ecological gradient, from high-altitude Himalayan lakes to coastal mangroves and inland floodplains, making them ideal for studying regional climate variability and ecosystem responses.

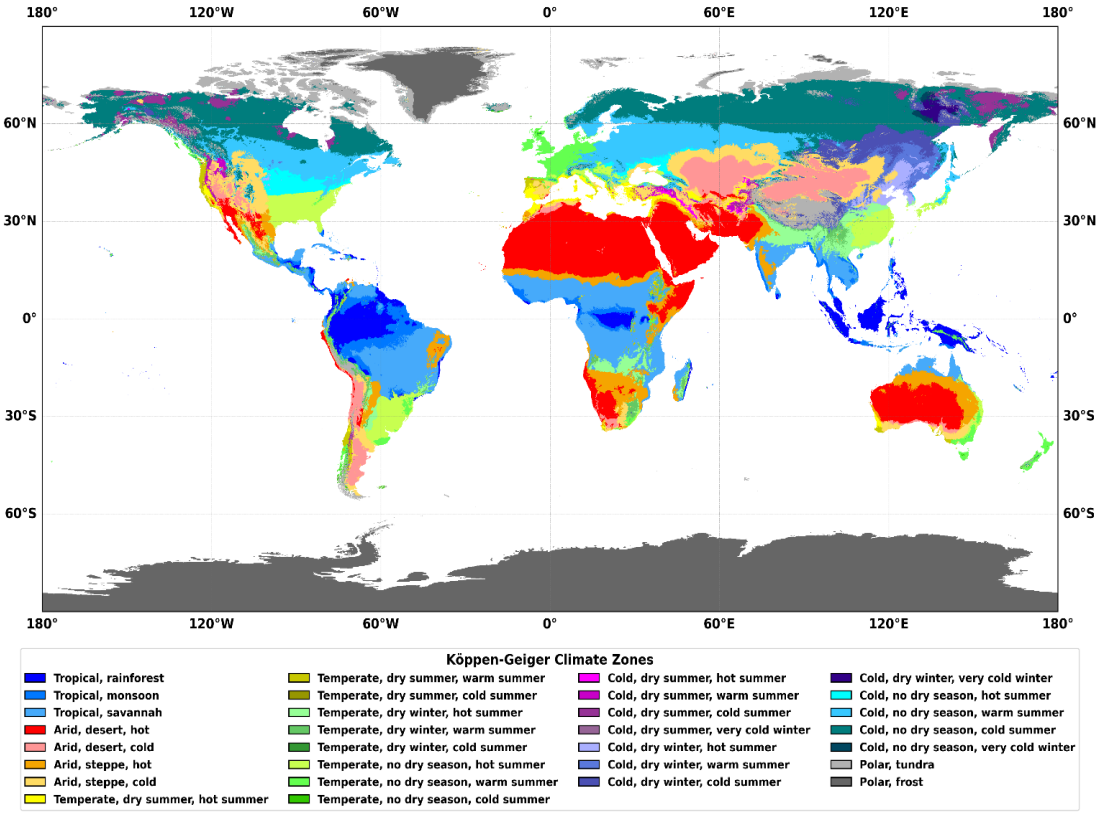

Figure 3: Köppen-Geiger climate classification (1991 - 2020).

Each wetland is shown in the colour corresponding to the Köppen-Geiger climate class it falls under, as per the legend in Figure *3*. This visualization links wetland locations with their prevailing climate regime for subsequent analysis.

The map depicts the 30 global climate zones derived from the updated Köppen-Geiger classification system, with the legend displaying the climate classes using Standardized color slabs for each zone (Beck et al., 2023, 2020). To integrate climatic context into our

analysis, each Ramsar site's climate region was determined by its geographic position, as defined by the Köppen-Geiger system. This widely recognized system categorizes the Earth's surface into 30 distinct climate zones based on temperature and precipitation patterns, enabling a standardized framework for assessing climatic influences across ecologically diverse sites, as in Figure 3.

The global scope of this study, combined with the ecological sensitivity and widespread distribution of Ramsar wetlands, offers valuable insights into climate change impacts across hydroclimatic regimes. These insights can support targeted adaptation strategies and inform international wetland conservation efforts. The Ramsar sites falling within respective Koppen-Geiger climate zones are visualized with distinct color codes representing their climate class, as shown in Figure 4.

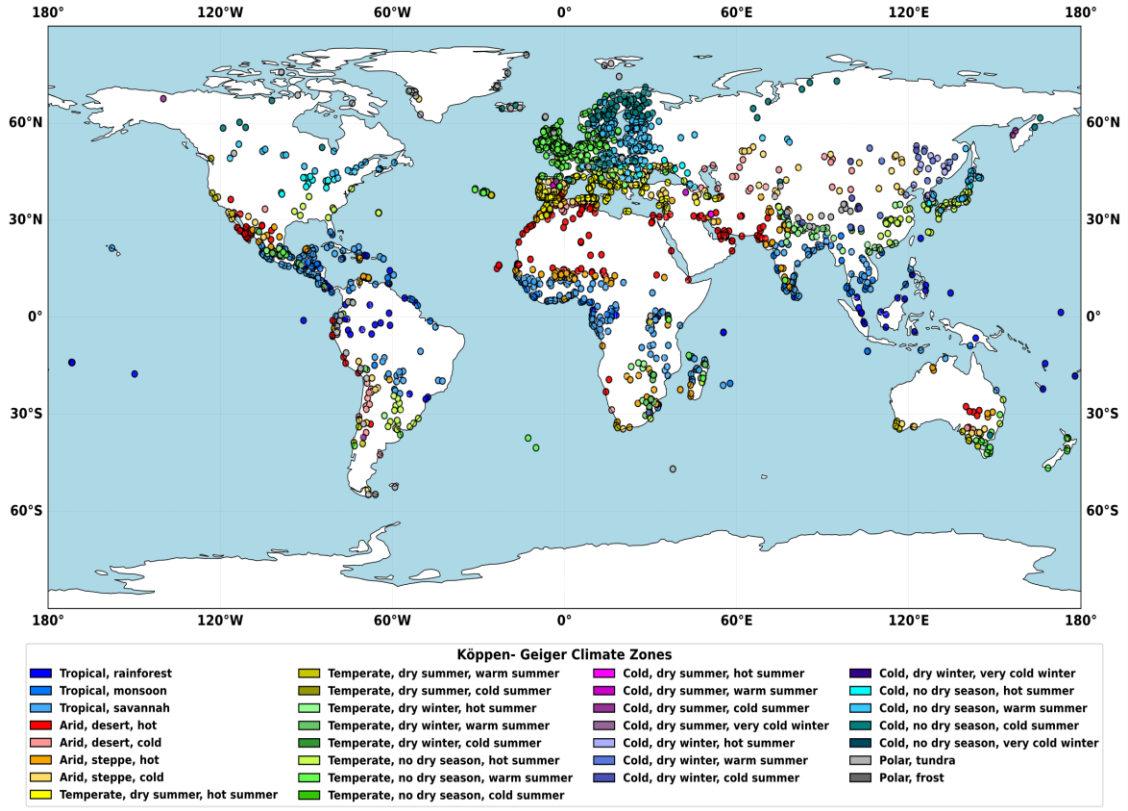

Figure 4: Ramsar wetlands are classified by climate zone.

4. Datasets & Methodology

To robustly assess the projected impacts of climate change on global Ramsar wetlands, this study utilizes high-resolution, bias-corrected climate datasets and a suite of established analytical techniques. By integrating multi-model climate projections with advanced metrics for precipitation variability and extremes, we ensure a comprehensive and reliable evaluation of hydrological risks across diverse wetland regions. The following section details the datasets employed and the methodological framework guiding this analysis.

4.1 Datasets

4.1.1 Precipitation Data

The NEX-GDDP-CMIP6 dataset is being used to assess climate change projected impacts across two different scenarios. Daily projections in this dataset have been statistically refined and corrected for bias, supporting climate analysis across a range of spatial scales, from local to regional (Thrasher et al., 2022, 2013, 2012). The projections are derived from the Coupled Model Intercomparison Project Phase 6 (CMIP6), which involves a large ensemble of General Circulation Models (GCMs) created by climate modeling institutions globally (Eyring et al., 2016, 2015; Simpkins, 2017). For this study, we specifically used daily precipitation data from 13 out of the 35 available GCMs (listed in Table 1) and computed Multi-model Ensemble mean (MME) for analysis. The precipitation variable used corresponds to the Climate Forecast (CF) standard name pr, which represents the average precipitation flux per day, quantified in kg m^{-2} s^{-1}. The analysis was carried out over two distinct periods: (1951 - 2024) and (2025 - 2100).

Public access to this dataset is provided through the NASA Centre for Climate Simulation (NCCS). Our study focused on two representative Shared Socioeconomic Pathways (SSPs): SSP 245 and SSP 585 (O'Neill et al., 2016; Meinshausen et al., 2020). These scenarios encompass a wide range of potential futures, considering factors such as greenhouse gas output, economic growth, patterns of energy consumption, and the extent of climate-related policy initiatives. SSP 245 outlines a moderate pathway characterized by incremental climate action and limited international collaboration. This scenario serves as an updated version of RCP4.5, reflecting more recent socioeconomic projections (Riahi et al., 2017). In contrast, SSP 585 describes a trajectory with substantial emissions, primarily

resulting from accelerated economic growth, a heavy reliance on fossil fuels (Dawson and Spannagle, 2020; IPCC, 2022, 2021; Kikstra et al., 2022) and an energy-intensive lifestyle (O'Neill et al., 2016). This scenario projects that radiative forcing of about 1.88 times the previous, consistent with the highest emission forecasts from earlier modeling efforts, including the 8.5 pathway (Meinshausen et al., 2011; van Vuuren et al., 2011).

Table 1: Details of the CMIP6 models incorporated into this study's analysis

Name of the model	Developing Institution	Country
ACCESS - CM2	CSIRO and ARCCSS	Australia
ACCESS - ESM1-5	CSIRO and ARCCSS	Australia
CNRM - CM6 – 1	CNRM - CERFACS	France
CNRM - ESM2 – 1	CNRM - CERFACS	France
EC - Earth3 – Veg - LR	Consortium-EC-Earth	Various countries
EC - Earth3	Consortium-EC-Earth	Various countries
IPSL - CM6A – LR	Institut Pierre-Simon Laplace	France
MIROC - ES2L	MIROC Project, University of Tokyo	Japan
MIROC6	MIROC Project, University of Tokyo	Japan
MPI - ESM1 - 2 – HR	Max Planck Institute for Meteorology	Germany
MPI - ESM1 - 2 - LR	Max Planck Institute for Meteorology	Germany
MRI - ESM2 - 0	Meteorological Research Institute	Japan
NESM3	National Earth System Model Team	China

To refine the spatial scale and correct for consistent biases in the unprocessed GCM data, the NEX-GDDP-CMIP6 resource adopts the Bias Correction Spatial Downscaling (BCSD) technique. This statistical downscaling method involves two main steps (Thrasher et al., 2022). First, bias correction is performed by adjusting the GCM data against a trusted observational baseline using quantile mapping (Maurer and Hidalgo, 2007). This approach maintains the statistical integrity of modeled data, and the occurrence and severity of

climate shifts correspond to the patterns documented in past climate data. The corrected data is spatially disaggregated to a high-detail grid at quarter-degree intervals (roughly 25 km). It is achieved using harmonic interpolation methods that incorporate local climatic patterns, thereby enhancing the fidelity of the data for local-scale studies.

The Global Meteorological Forcing Dataset (GMFD), produced by Princeton University, served as the reference dataset for bias correction (Lange and Büchner, 2020). The GMFD combines reanalysis data with observational records to produce reliable, continuous daily measurements of climate parameters such as air temperature, rainfall, wind, moisture content, and incoming solar energy (Wood et al., 2004). The temporal coverage of this dataset extends from 1960 to 2014 and is gridded at the same resolution (0.25^0) as the downscaled projections, making it well-suited for the bias correction process. It is used as the standard reference for aligning and adjusting the historical climate model outputs.

Overall, the NEX-GDDP-CMIP6 dataset provides a comprehensive and high-resolution view of possible future climate conditions under different emission pathways. Its daily temporal resolution and spatial granularity allow for detailed impact assessments, especially in regions with complex topography or high climate sensitivity. The inclusion of both moderate and high-emission scenarios in this study offers insights into a range of potential futures, supporting more informed decision-making for climate adaptation and mitigation efforts.

4.2 Variability and Extremes Methodology

To assess the temporal and spatial variability of precipitation, we employed statistical techniques that quantify fluctuations in rainfall over different timescales. Metrics such as the standard deviation and entropy-based indices were used to characterize the degree of variability, following established approaches in climate science (Hobeichi et al., 2024; Pendergrass et al., 2017). It allows for the identification of regions and periods exhibiting significant departures from average conditions, which is crucial for understanding the hydrological sensitivity of wetlands under changing climate regimes.

Extreme precipitation events, including both intense rainfall and prolonged droughts, are key drivers of water-related processes and the robustness of wetland habitats. In this study, we analyzed a suite of indices given by ETCCDI to analyze the prevalence, frequency, and duration of precipitation shifts (Li et al., 2024; Maimone et al., 2023). These indices were

calculated for both historical and projected periods, enabling a detailed examination of how the rate at which extreme events happen and their degree of severity may evolve under different climate scenarios.

4.2.1 Precipitation Variability

(Shannon, 1948) introduced the metric "Entropy," which is used to assess the degree of uncertainty, randomness, or disorder in a random variable. When applied to precipitation data, entropy provides a quantitative measure of how variable and unpredictable rainfall is across different locations and periods, effectively capturing the complexity within the precipitation time series. The discrete $\boldsymbol{S(v)}$ entropy for a random variable V is given in Equation (i)

$$S(V) = -\sum_{r=1}^{R} k(v_r) \log_2 k(v_r) \qquad \text{(i)}$$

In this equation, $k(v_r)$ represents the likelihood of the r^{th} event and R denotes an entire count of potential events. Entropy attains its peak value when all events occur with equal probability, indicating the highest level of unpredictability. The metric spans from 0 (absolute predictability) to $\log_2 R$, reflecting the system's inherent randomness.

In hydrological applications, entropy is a valuable tool for assessing variability within precipitation time series across different temporal and spatial scales (Kawachi et al., 2001). This study applies entropy analysis using three specific measures

4.2.2 Marginal Entropy ($\boldsymbol{ME}$)

$\boldsymbol{ME}$ measures unpredictability or disorder level within an individual time series, reflecting how values fluctuate over time (Cheng et al., 2017; Darbandsari and Coulibaly, 2022; de P. Rodrigues da Silva et al., 2016; Mishra et al., 2009). Employed to evaluate temporal variability in rainfall distributions across varying time scales, focusing on monthly and annual periods, at Ramsar wetland locations. It is calculated as shown in Eq. (ii)

$$ME = -\sum_{t=1}^{N} \frac{q_t}{Q} \log_2 \left(\frac{q_t}{Q}\right) \qquad (ii)$$

Here, q_t represents the precipitation recorded during the t^{th} interval (such as a specific month or year), Q denotes the cumulative rainfall over the dataset's full duration, and N

refers to the entire count of intervals considered (for example, the total count of months or years in the study period).

4.2.3 Apportionment Entropy (*AE*)

The entropy-based metric ***AE*,** is introduced to gauge how evenly a specific variable is allocated or spread out. Measures how total rainfall is distributed over individual months or seasons, providing insights into how consistently rainfall occurs over different periods, calculated as shown in Eq. (iii)

$$AE = -\sum_{m=1}^{p} \frac{e_m}{P_T} \log_2 \left(\frac{e_m}{P_T}\right) \quad \text{(iii)}$$

Where e_m is the rainfall amount in the m^{th} period (e.g., month or season). P_T is the total annual rainfall. p represents the total count of discrete time units, such as months or seasons, within the time series (Maruyama et al., 2005).

4.2.4 Standardized Variability Index

Redundancy metric ***SVI*** by (Singh, 2013) is applied here to investigate repetition and predictability patterns across multiple timescales and regions, ***SVI*** was applied as shown in Eq. (iv)

$$SVI = \frac{S_{max} - S_{val}}{S_{max}} \quad \text{(iv)}$$

Where $\boldsymbol{S_{val}}$ is the calculated entropy and $\boldsymbol{S_{max}}$ is the maximum possible entropy for that series. SVI ranges from 0 (no variability, maximum certainty) to 1 (maximum variability, maximum uncertainty), enabling consistent comparison across regions (Guntu et al., 2020a; Rolim et al., 2022). Particularly useful for assessing variability over multiple temporal scales, this index provides a consistent framework for measuring uncertainty. Its bounded range supports meaningful comparisons across datasets with varying lengths, making it suitable for regional analyses (Choobeh et al., 2024). 13-time series comprising monthly (12 months) and annual data (1 series) were used to capture and compare precipitation variability across different temporal resolutions.

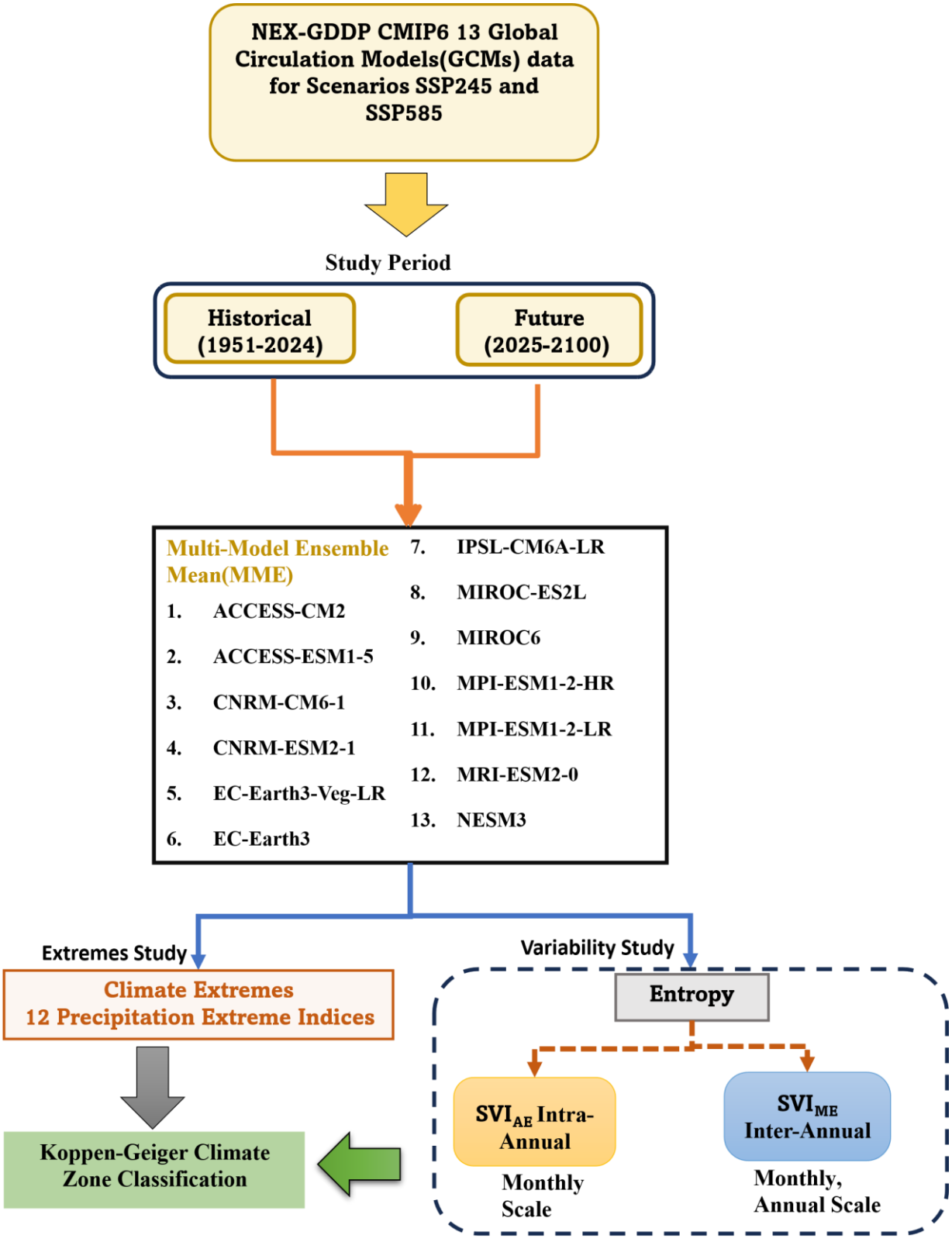

Figure 5: Methodology Flowchart

4.2.5 Extremity Indices

The research utilized twelve indices based on extreme rainfall derived from the Standardized framework established by ETCCDI, coordinated by WMO in cooperation with both CLIVAR and JCOMM (Karl et al., 1999). These indices serve as globally accepted methods for evaluating variations in how often, how severe, and how long extreme precipitation events occur (Bobde et al., 2024; Donat et al., 2016; Yin and Sun, 2018). Twelve key indices were selected for this analysis, for instance, the frequency of intense rainfall days (R10mm), the occurrence of exceptionally heavy rain events (R20mm), the Simple Daily Intensity Index (SDII), peak single-day precipitation totals (Rx1day), highest accumulated rainfall over five consecutive days (Rx5day), stretches of successive wet days (CWD), yearly precipitation sums (PRCPTOT), and measures reflecting the proportion of rainfall from very wet (R95pTOT) and extremely wet days (R99pTOT), along with frequency-based metrics (RR95, RR99) and total rainy days (RD). The selection reflects their global prominence and relevance for hydrological and climatic impact assessments in the study region (Wilson et al., 2022). Each index was computed annually across 2,490 wetland sites using simulations from multiple CMIP6 climate models, covering both historical and future climate scenarios. By aggregating individual model outputs into a multi-model ensemble mean (MME), the analysis reduces model-specific biases, yielding a more reliable characterization of extreme precipitation patterns (Figure 5).

Table 2: Precipitation Extremes Metrics Considered

ID	Index Name	Definition	Units
RD	Number of Rainy Days	Total number of days per year with precipitation ≥ 1 mm	days
CWD	Consecutive Wet Days	Maximum number of consecutive days with precipitation ≥ 1 mm	days
R95pTOT	Very Wet Day Contribution	Annual total precipitation from days ≥ 95th percentile threshold	mm
RR95	Number of Very Wet Days	Number of days per year with precipitation ≥ 95th percentile	days
Rx1	Maximum 1-Day Precipitation	Highest daily precipitation in a year	mm
SDII	Simple Daily Intensity Index	Annual mean precipitation per wet day (precipitation ≥ 1 mm)	mm/day

Calculating these indices on an annual basis ensures effective tracking of interannual variability and long-term trends (Avila-Diaz et al., 2020). Understanding how extreme

precipitation patterns may shift in the future is essential for effective planning and management of regional water resources. Insights into these changes directly inform the development of robust adaptation strategies, helping communities and policymakers design measures that enhance resilience to climate-related water challenges (Eekhout et al., 2018; Elgendy et al., 2024; Karl et al., 1999; Rogers et al., 1996; Zhang et al., 2011; Zhao and Boll, 2022).

5. Results

This section comprehensively analyses projected changes in precipitation variability and extremes across global Ramsar wetlands under different climate scenarios. By examining both intra- and inter-annual variability as well as a suite of extreme precipitation indices, we identify emerging patterns, regional contrasts, and site-specific responses in wetland hydrology. The results highlight how climate change may reshape the distribution and intensity of hydrological extremes, with significant implications for wetland resilience and ecosystem functioning.

5.1 Entropy Study

5.1.1 Intra-Annular variability SVI_{AE} at monthly scale

Under the SSP 245 scenario, a comparison between the historical period (1951 - 2024) (a) of Figure 6 and the future period (2025 - 2100) (b) of Figure 6 reveals evolving patterns in precipitation variability across global Ramsar sites. The number of wetlands classified under medium variability increases modestly from 239 to 255, suggesting a growing number of sites are becoming more sensitive to monthly-scale precipitation fluctuations. The high variability category continues to be dominated by a single site, Oasis du Kawar, in Algeria, which lies within the arid, desert, hot climate zone according to the Koppen-Geiger classification (BWh). Meanwhile, low variability sites decline slightly from 2,247 to 2,234, indicating a gradual redistribution from stable to more variable conditions and highlighting a potential increase in the responsiveness of these ecosystems to changing climate signals.

The figure demonstrates the intra-annual variability along the Ramsar sites globally for different scenarios: (a) SSP 245 historical, (b) SSP 245 future, (c) SSP 585 historical, and (d) SSP 585 future. Under the SSP 585 scenario, the shift toward elevated variability becomes more pronounced. Medium variability sites increase from 241 to 260, reflecting a broader emergence of wetlands experiencing intensified precipitation variability. Oasis du Kawar remains the sole site in the high variability class in the future period, underscoring its persistent climatic instability under extreme emissions scenarios. Low variability sites decrease further from 2,246 to 2,229, representing a more substantial redistribution compared to SSP 245. This trajectory under the high-emissions pathway indicates that more

wetlands may transition from stable to variable regimes, driven by the amplification of hydrological extremes.

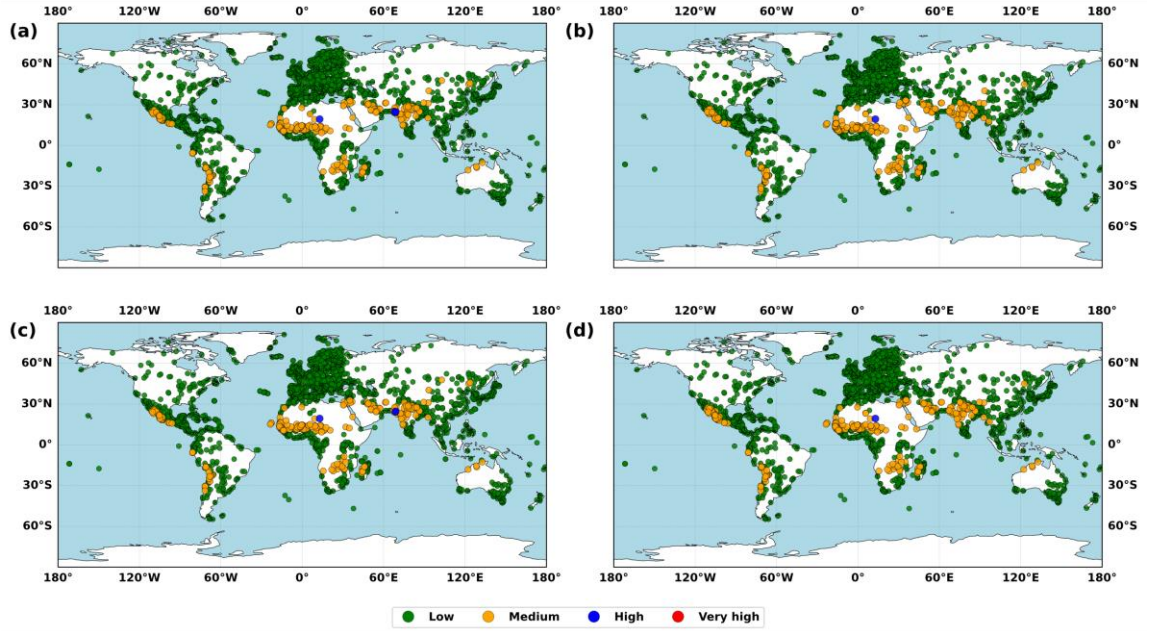

Figure 6: SVI_{AE} monthly variability (Intra-annual).

Historical variability distributions are nearly identical between the two scenarios. SSP 245 includes four sites in the high variability class, while SSP 585 includes 3 (c) in Figure 6. Medium and low variability site counts differ only slightly, indicating a broadly similar baseline distribution across scenarios before future changes.

Future projections under both scenarios converge with Oasis du Kawar remaining in the high variability class. However, (d) in Figure 6 SSP 585 results in a more pronounced increase in medium variability sites compared to SSP 245. It suggests that greater emissions forcing may enhance the redistribution of sites into higher variability categories. The accompanying reduction in low variability sites, although minor, supports this pattern.

Taken together, the most consistent signal across both climate pathways is the increase in medium variability of wetlands. While high variability remains uncommon, the growth in medium-class sites underscores a fundamental shift in precipitation behavior at a monthly scale. Wetlands historically characterized by stable conditions are now projected to experience more dynamic hydrological variability, with potential implications for seasonal balance and ecological functioning.

5.1.2 Inter-Annual variability SVI_{ME} at a monthly scale

In the SSP 245 historical scenario, February consistently exhibited the highest concentration of Ramsar sites in the very high variability category, with 74 sites globally, including 66 sites in an arid desert, a hot climatic zone of Africa, and Eight Ramsar-designated wetlands in Asia situated within regions characterized by arid and steppe climates, as well as areas experiencing hot and temperate conditions with dry winters and hot summers. Interestingly, October recorded 1 Ramsar site in this category, located in Africa. The high variability category showed considerable seasonal variation, with the highest count in December (16 sites) and the fewest in March (0 sites). The medium variability category peaked in November (33 sites), while April, June, and September had the fewest sites (11 sites each). As for the low variability category, February recorded the fewest sites globally (2,398 sites), the largest concentration found in Europe, with 1,094 designated wetlands primarily situated in temperate zones characterized by warm summers and no distinct dry season, while Oceania has the fewest such sites (81 sites). In contrast, March had the highest number of low variability sites globally (2,468 sites), as shown in Figure 7.

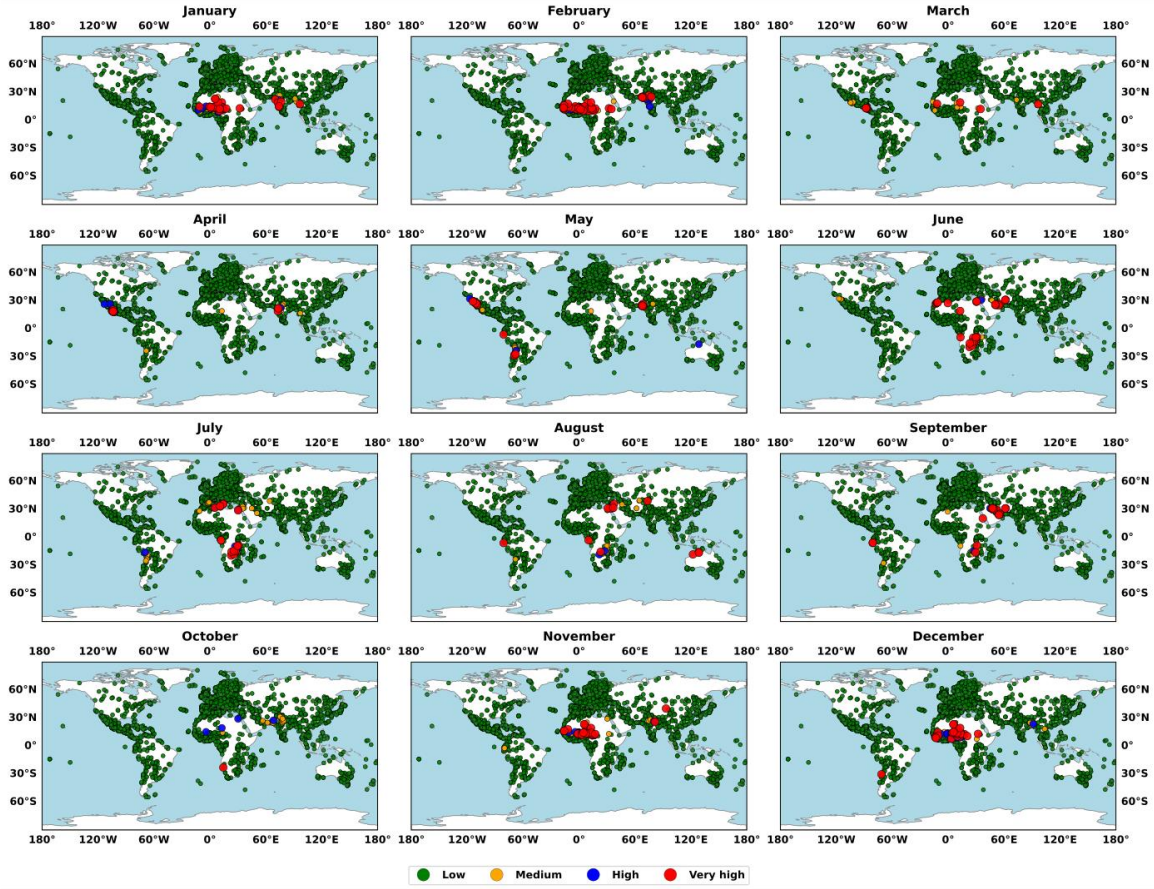

Figure 7: Inter-annual variability SVI_{ME} at a monthly scale for SSP 245 Historical (1951-2024).

The index values are divided into four classes mentioned in the legend: green for low ($0 \leq SVI_{ME} \leq 0.25$), yellow for medium ($0.25 < SVI_{ME} \leq 0.5$), blue for high ($0.5 < SVI_{ME} \leq 0.75$), and red for very high variability ($0.75 < SVI_{ME} \leq 1$).

For future projections of SSP 245, the distribution of sites with very high variability will remain similar to historical patterns. February continued to feature 74 Ramsar sites classified as very high variability, with the distribution between Africa (66 sites) and Asia (8 sites) unchanged from the same climatic zones mentioned for SSP 245 historical. The high variability class increased slightly, with 16 sites in November and additional sites in February, May, June, and October. The medium variability category peaked in November (34 sites), while September recorded the fewest sites in this category (8 sites). The low variability category was again most prominent in February (2,393 sites) and October (2,471 sites), as shown in Figure 8.

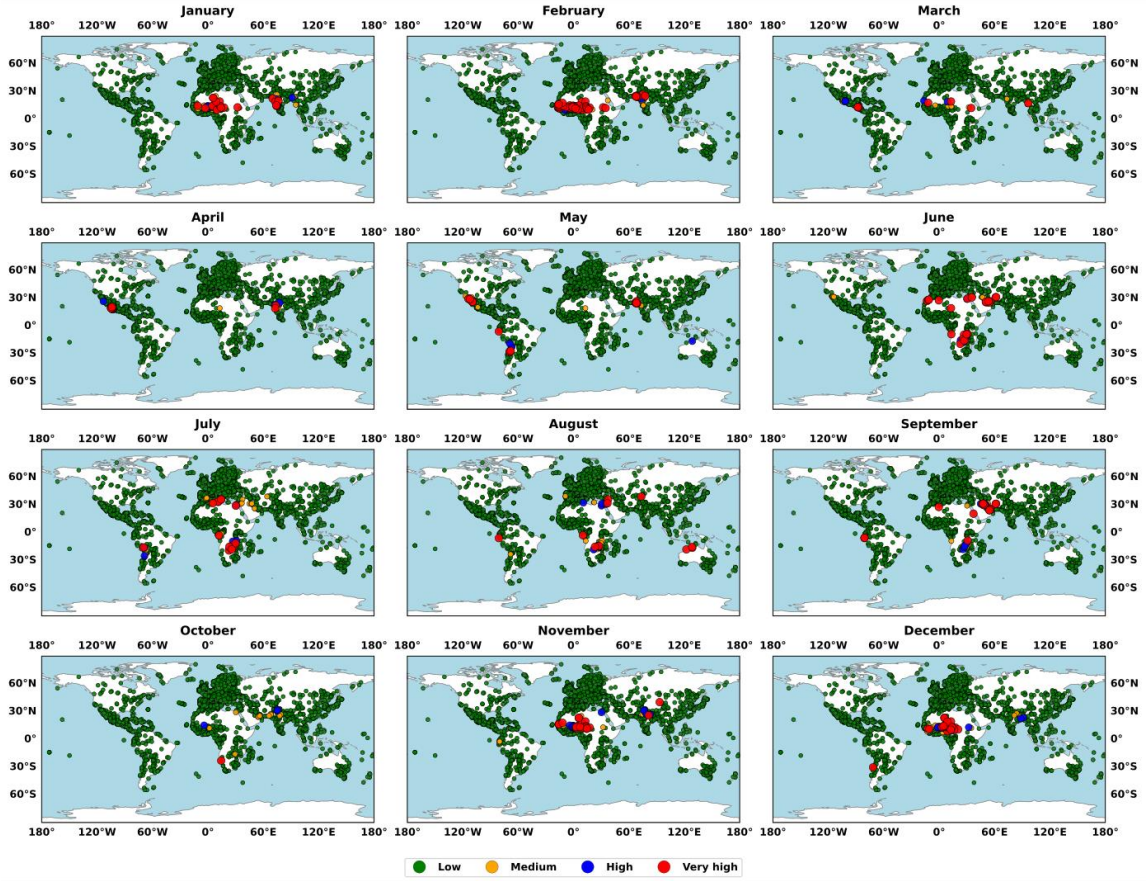

Figure 8: Inter-annual variability SVIME at a monthly scale for SSP 245 future (2025-2100).

The index values are divided into 4 classes mentioned in the legend: green for low ($0 \leq SVI_{ME} \leq 0.25$), yellow for medium ($0.25 < SVI_{ME} \leq 0.5$), blue for high ($0.5 < SVI_{ME} \leq 0.75$), and red for very high variability ($0.75 < SVI_{ME} \leq 1$) for 12 months.

In the SSP 585 historical scenario, trends were similar to SSP 245. February remained the month with the most Ramsar sites in the very high variability category (74 sites: 66 in Africa, 8 in Asia). October recorded 2 sites in the very high category, both located in Africa. The high variability category reached its maximum in December (16 sites), with March showing the lowest count (0 sites). In November, the medium variability category peaked at 35 sites (Africa contributed 23 sites, Asia 9 sites, and South America 3 sites). The low variability category had a maximum of 2,471 sites in March and a minimum of 2,397 sites in February, as shown in Figure 9.

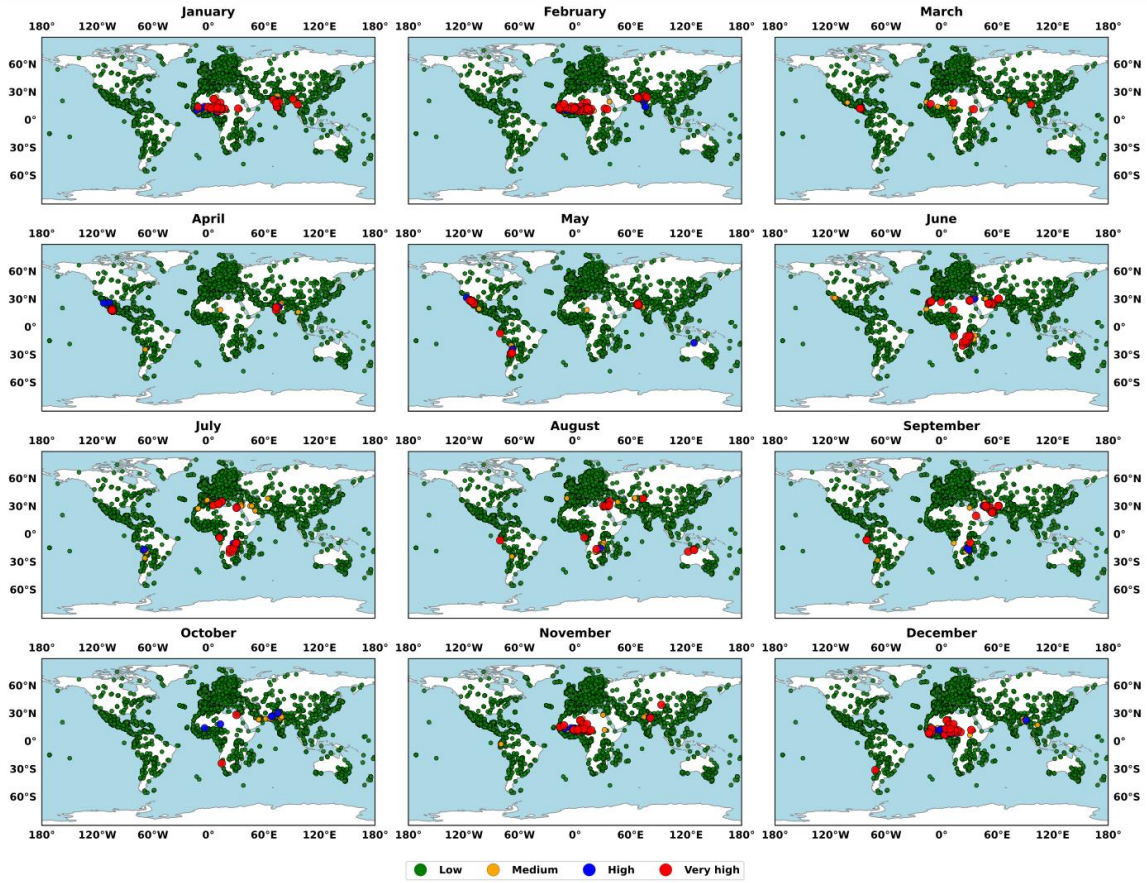

Figure 9: Inter-annual variability SVI_{ME} at a monthly scale for SSP 585 Historical (1951-2024).

The index values are divided into 4 classes mentioned in the legend: green for low ($0 \leq SVI_{ME} \leq 0.25$), yellow for medium ($0.25 < SVI_{ME} \leq 0.5$), blue for high ($0.5 < SVI_{ME} \leq 0.75$), and red for very high variability ($0.75 < SVI_{ME} \leq 1$) for 12 months. For the future projections of SSP 585, the very high variability category saw a slight increase to 75 sites

in February (66 in Africa, 9 in Asia). One site was recorded in Africa in October. The high variability category peaked at 16 sites in July, with 11 sites in Africa, 1 site in Asia, 3 sites in Europe, and 1 site in South America. March recorded the minimum (1 site in Africa). The medium variability category peaked at 27 sites in November, with 14 sites in Africa and 13 sites in Asia. Low variability remained the dominant category, peaking in October (2,472 sites) and February (2,395 sites), as shown in Figure 10.

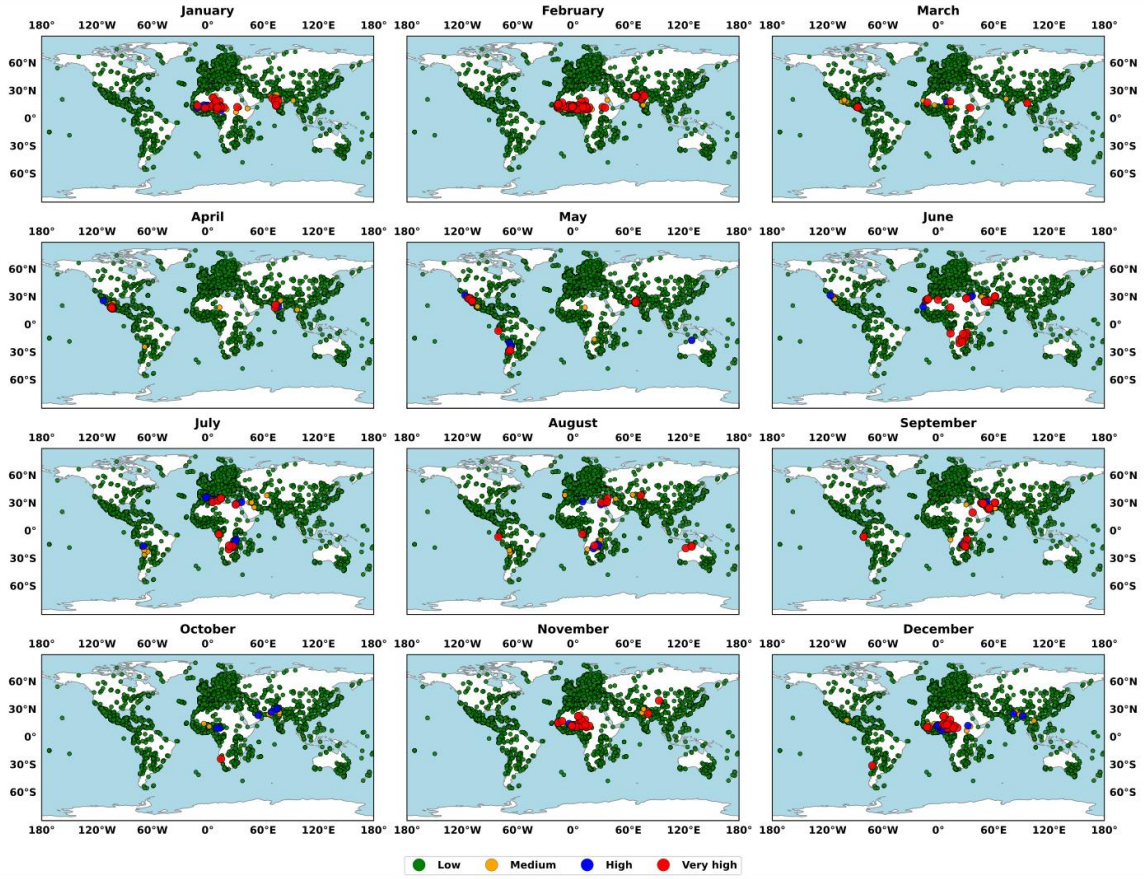

Figure 10: Inter-annual variability SVI_{ME} at a monthly scale for SSP 585 future (2025-2100).

The index values are divided into 4 classes mentioned in the legend: green for low ($0 \leq SVI_{ME} \leq 0.25$), yellow for medium ($0.25 < SVI_{ME} \leq 0.5$), blue for high ($0.5 < SVI_{ME} \leq 0.75$), and red for very high variability ($0.75 < SVI_{ME} \leq 1$) for 12 months. Regarding site-level shifts in SVI_{ME}, Nguru Lake and the Marma Channel Complex of the arid, steppe hot zone of Africa recorded a significant increase in SVI_{ME} in October, shifting dramatically within the low variability category. Fivebough and Tuckerbil Swamps in the arid, steppe, cold zone of Oceania showed a slight increase in SVI_{ME} in November, remaining within the low variability category. Being in a temperate, dry summer, hot summer zone, Zarivar in Asia experienced a notable decrease in SVI_{ME} in August, transitioning from medium to

low variability. Kayrakum Reservoir, also in Asia, falling under the arid, desert, cold zone, showed a minor decrease in SVI_{ME} in November, remaining in the low category.

Under SSP 585, Nguru Lake and the Marma Channel Complex showed a remarkable shift in SVI_{ME} in October, transitioning from low to high variability. Conversely, the Angola Accession Site in Africa had a very minor increase in SVI_{ME} in May, reflecting almost no change in variability. The most dramatic decrease in SVI_{ME} under SSP 585 occurred at Île Blanche, another African site falling in the tropical monsoon climate zone, which saw a significant drop in December, transitioning from high to low variability. Annsjön in Europe experienced a slight decrease but remained in the low variability category.

5.1.3 Inter - Annual variability SVI_{ME} at the annual scale

At the annual scale, the analysis of SVI_{ME} under SSP 245 reveals remarkable stability in categorical variability across both historical (1951 - 2024) (a) in Figure 11 and future (2025 - 2100) (b) in Figure 11 periods. Of the 2,490 Ramsar sites studied, only one site, Delta Intérieur du Niger (Mali), exhibited medium variability in both timeframes, showing a decrease in entropy index from 0.335 during the historical timeframe to 0.2899 in the projected future, a modest reduction. The remaining 2,489 sites consistently retained low variability classification across both periods. Despite this constancy in class distribution, entropy values within the low variability category exhibited both upward and downward trends. Specifically, 1,091 sites demonstrated entropy increases, ranging from a minimal increment at Pelican Island National Wildlife Refuge (USA) to a significant rise at East Calcutta Wetlands (India). Notably, East Calcutta Wetlands showed scenario-sensitive behavior, with entropy declining under SSP 585.

Entropy measurements dropped at 1,399 sites under SSP245, signaling reduced variability between baseline and future climate conditions. Most of the extreme reduction occurred at the Sierra Leone River Estuary (Sierra Leone), with entropy falling sharply, while the least decline was observed at Lavinia Nature Reserve (Australia), showing a negligible decrease. These results illustrate that even though class-level variability remained constant, internal dynamics at the entropy value level reveal nuanced responses to climate forcing across individual sites.

Under SSP 585, similar categorical consistency was observed. Delta Intérieur du Niger remained the only site in the medium variability class, with entropy declining from 0.3418

to 0.271. All remaining 2,489 sites retained low variability classification across historical and future periods represented in (c) and (d) in Figure 11. However, entropy magnitudes displayed a sharper contrast compared to SSP 245. A total of 1,937 sites exhibited increased entropy values under SSP 585, with the most dramatic increase occurring at Maladumba Lake (Nigeria), highlighting high sensitivity to emissions trajectory. Interestingly, this same site showed an opposite trend under SSP 245.

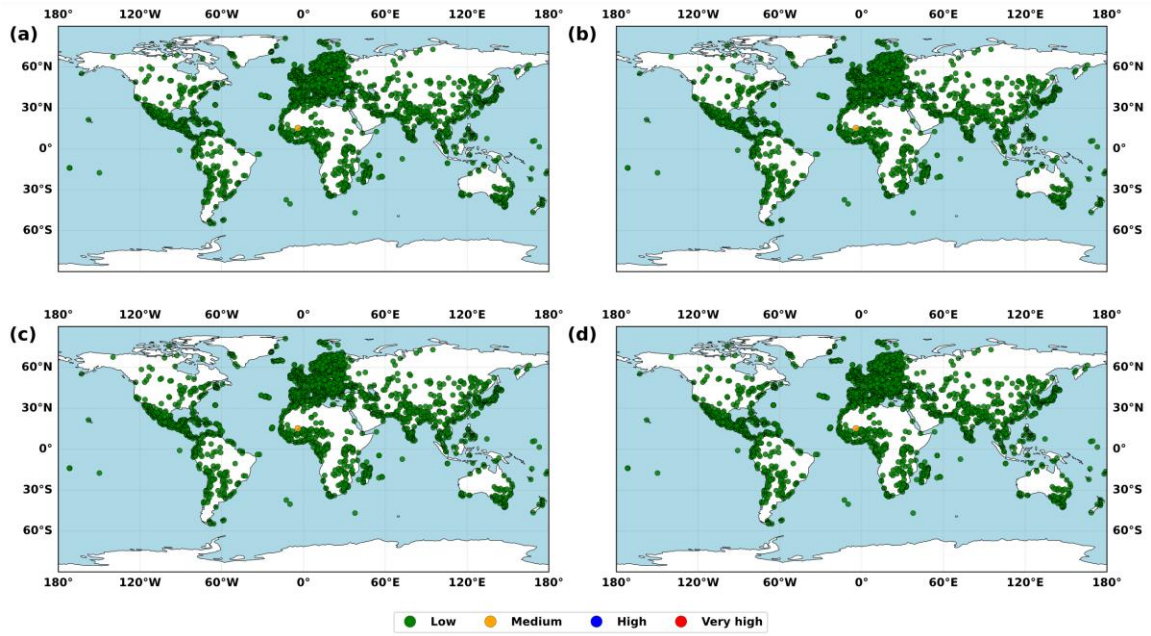

Figure 11: Inter-annual variability SVI_{ME} at the annual scale.

The index value is categorized into 4 classes at 4 different scenarios across 2 different time durations: (a) SSP 245 historical (1951-2024), (b) SSP 245 future (2025-2100), (c) SSP 585 historical (1951-2024), (d) SSP 585 future (2025-2100). Entropy decreased in 553 sites under SSP 585. The most substantial decline was again seen at Sierra Leone River Estuary (tropical, monsoon climate zone), closely mirroring the drop observed in SSP 245. The least decrease was recorded at Thanet Coast and Sandwich Bay (England), where entropy reduced marginally. Intriguingly, this same site registered a significant increase under SSP 245, reinforcing the site-specific variability in response to scenario pathways.

Crucially, across both SSP 245 and SSP 585, despite the extensive spread of entropy increases and decreases at the site level, the number of Ramsar sites in each variability class (medium and low) remained identical between historical and future periods. It includes Delta Intérieur du Niger (Mali), which maintained its medium variability status in all cases, despite undergoing reductions in entropy and is present in arid, desert, hot climate zone.

This categorical stability, even amidst substantial numerical shifts in entropy values, suggests that while overall annual-scale variability is not dramatically reorganized in class terms, the internal dynamism within classes is substantial and, in some sites, highly sensitive to emissions scenario and regional hydrological response.

5.2 Spatiotemporal Analysis of Precipitation Extremes across Ramsar Sites

Twelve key precipitation indices are analysed under four scenarios, encompassing both historical and projected periods for the SSP 245 and SSP 585 emission pathways to evaluate spatial and temporal variations in precipitation extremes under changing climate conditions. These indices, R10, R20, RD, CWD, PRCPTOT, R95pTOT, R99pTOT, RR95, RR99, Rx1, Rx5, and SDII, characterize how often precipitation events occur, how intense they are, and how long they last, including the most extreme rainfall episodes. For each scenario, spatial plots represent the global distribution of these indices, enabling comparison between moderate and high-emission pathways over time. This framework provides a basis for assessing regional changes in rainfall behavior and identifying potential climate risks. Under SSP 245 historical conditions, there are notable differences in how precipitation extremes are distributed geographically among the six zones. In Asia, wetlands experience intense short-duration rainfall, with Rx1 ranging between 80 - 120 mm and SDII between 7 - 11 mm/day. The CWD spans between 20 and 45 days, while RD can extend to 180 days in arid sub-regions. Very wet days (RR95) occur 12 - 25 times annually, contributing to a substantial share (18 - 28%) of total annual rainfall through R95pTOT. In Africa, particularly across Central and West Africa, rainfall is both intense and unevenly distributed. Rx1 varies from 70 - 110 mm, and SDII values are relatively high (8 - 12 mm/day).

CWD reaches up to 40 days, and RD can last as long as 200 days in some regions. The RR95 varies from 10 to 22, and the proportion of total precipitation (R95pTOT) attributed to these days is remarkably high, reaching 20 - 30%. Europe shows moderate precipitation extremes with Rx1 in the range of 60 - 100 mm and SDII between 6 - 9 mm/day. However, it experiences extended wet spells, with CWD reaching up to 50 days. RR95 ranges from 8 - 18 events per year, and R95pTOT remains within 12 - 20%, suggesting a relatively lower concentration of extremes compared to tropical regions. In North America, Rx1 ranges from 65 - 110 mm and SDII from 7 - 10 mm/day. Wetlands experience 15 - 35 CWD

and RD extending up to 180 days in drier areas. The RR95 varies from 10 - 20, while 14 - 24% of total rainfall originates from these extreme events R95pTOT.

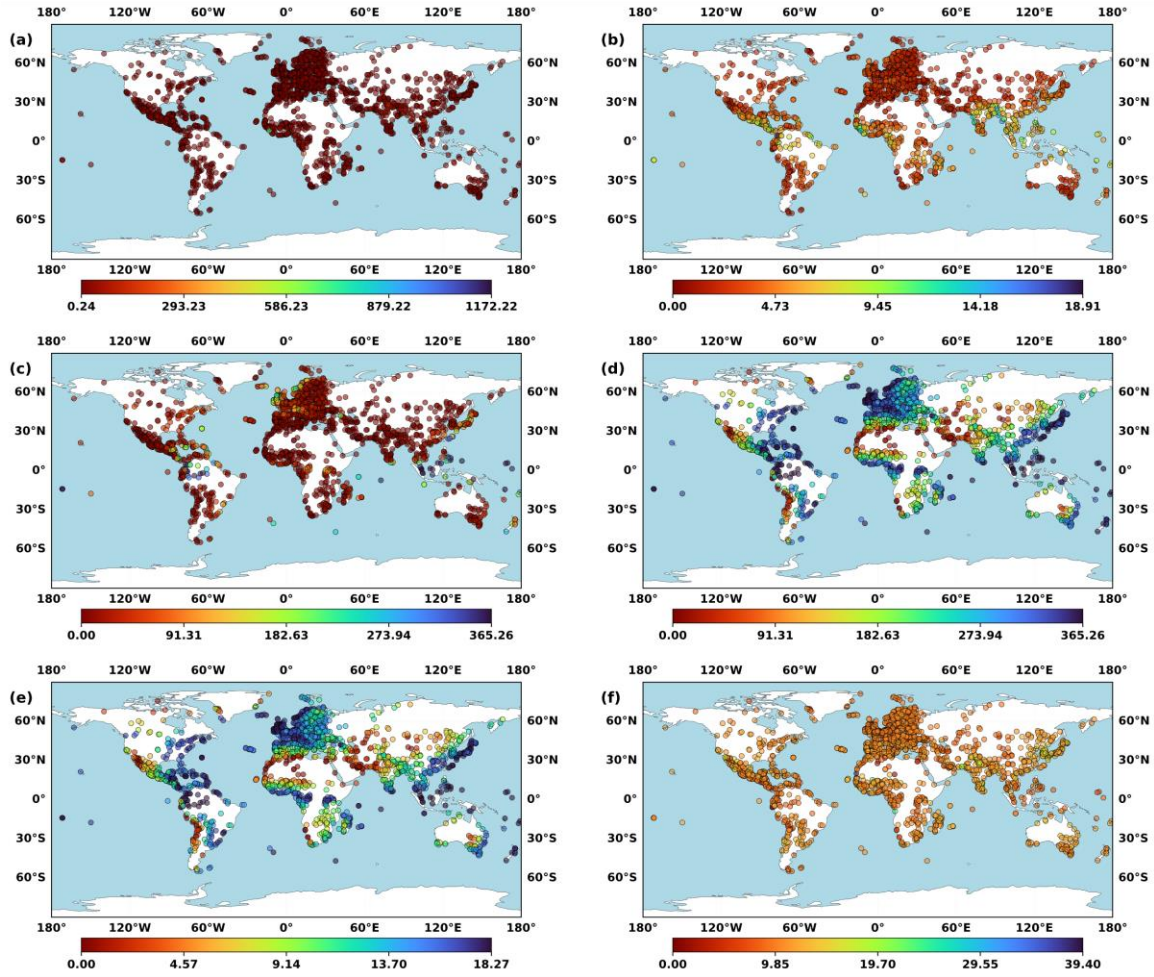

Figure 12: Geographical patterns of precipitation extremes indices in global wetlands during the historical SSP 245 scenario (1951 - 2024).

Rx1 exceeds 130 mm within specific parts of Asia, including the western coastal belt of Southern America, represented in deep red shades (a), while SDII reaches up to 20 mm/day in Africa and Southeast Asia, indicated by purple (b). CWD surpasses 60 in Europe and parts of South America (c), highlighted in dark violet, and RD exceeds 300 in equatorial Africa and Southeast Asia (d), shown in bright red. Very wet days (RR95) occur more than 28 times annually across Asia and the Amazon Basin (e), shown in red and yellow, while areas within the Congo Basin and the Amazon region (f) record R95pTOT values above 35% of total precipitation, highlighted in brown in Figure 12. Particularly, the Amazon basin is characterized by high Rx1 values (75 - 115 mm), with SDII between 8 - 11 mm/day.

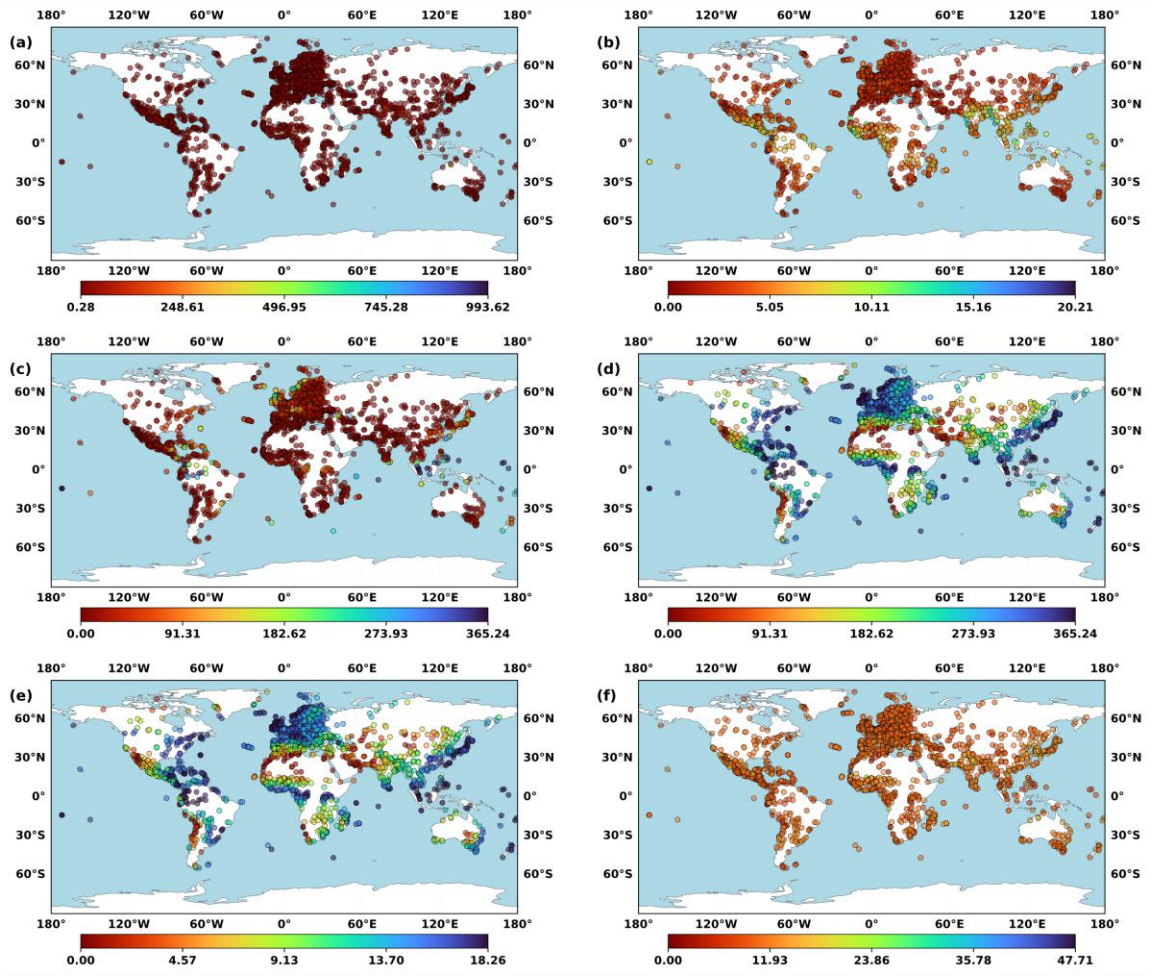

Figure 13: Geographical patterns of precipitation extremes indices in global wetlands during the future SSP 245 scenario (2025 - 2100).

Wet periods extend up to 40 days, while RR95 occurs 12 - 22 times annually. R95pTOT exceeds 25% in several tropical wetlands, indicating significant rainfall clustering. Oceania demonstrates moderate precipitation behavior with Rx1 ranging from 60 - 90 mm and SDII from 6 - 9 mm/day. CWD ranges from 15 - 35 days, while RD extends up to 190 days, especially in parts of Australia. RR95 occurs 8 - 16 times per year, and R95pTOT is between 13 - 21%. Finally, the Global Tropics emerge as the most hydrologically extreme zone, with Rx1 exceeding 130 mm, SDII between 9 - 13 mm/day, CWD reaching 45 days, and RR95 occurring up to 28 times annually. Notably, more than 25 - 35% of total precipitation in this region is delivered by very wet days, underscoring the severe clustering of rainfall extremes in tropical wetland systems.

Rx1 surpasses 140 mm within specific parts of Asia, including the western coastal belt of Southern America, with these zones depicted in deep red (a), while SDII reaches up to

20 mm/day in Africa and Asia, shown in purple (b). CWD surpasses 60 in Europe and North Asia (c), indicated by dark violet, and RD exceeds 300 annually in Central Africa and Southeast Asia, marked in red (d). RR95 occurs over 28 times/year in South America and Asia (e), shown in red and yellow, while R95pTOT exceeds 40% in several African and Amazonian sites (f), highlighted in brown. Under the SSP 245 future scenario (2025 - 2100) in Figure 13, wetlands across the globe are projected to undergo intensifying hydrometeorological extremes, though with marked regional contrasts in severity and expression. Asia, South America, and the Global Tropics are projected to face the most dramatic escalation, with Rx1 values exceeding 140 - 150 mm, SDII reaching 10 - 13 mm/day, and RR95 occurring up to 30 times annually. These regions also exhibit the highest rainfall concentration, with R95pTOT contributing 28 - 38% of annual precipitation, suggesting that rainfall is increasingly clustered into a small number of high-impact events, heightening flood risk and overwhelming wetland buffering capacities. In Africa, the dual stress of high-intensity rainfall (Rx1: 90 - 130 mm; SDII: 9 - 13 mm/day) and RD extending up to 180 days reflects a growing seasonal imbalance. RR95 values in African wetlands range from 13 - 25 days/year, with a significant share of rainfall (22 - 32%) concentrated in those events. North America shows similar signs of intensification, with Rx1 reaching 120 mm, SDII up to 11 mm/day, and extreme days contributing up to 28% of annual rainfall, particularly affecting western and southern wetland systems. In Europe, changes are more moderate but still notable: CWD lengthen to 50 days, and rainfall intensity (SDII: 7 - 10 mm/day) increases steadily, while R95pTOT remains below 22%, signaling a gradual but persistent shift in precipitation patterns. Oceania, particularly Australia, experiences moderate extremes, with Rx1 reaching 105 mm, wet spells lasting 20 - 35 days, and dry spells persisting up to 170 days, indicating an episodic and uneven wet-dry cycle. Across all regions, however, the Global Tropics remain the epicenter of hydrological intensification, with nearly every index reaching its upper bound, including Rx1 >150 mm, SDII >13 mm/day, and extreme rainfall days delivering more than 38% of annual precipitation. These findings collectively highlight a growing reliance on extreme precipitation events to fulfill annual hydrological budgets in wetlands worldwide, threatening not only their ecological balance but also their resilience under projected climate trajectories.

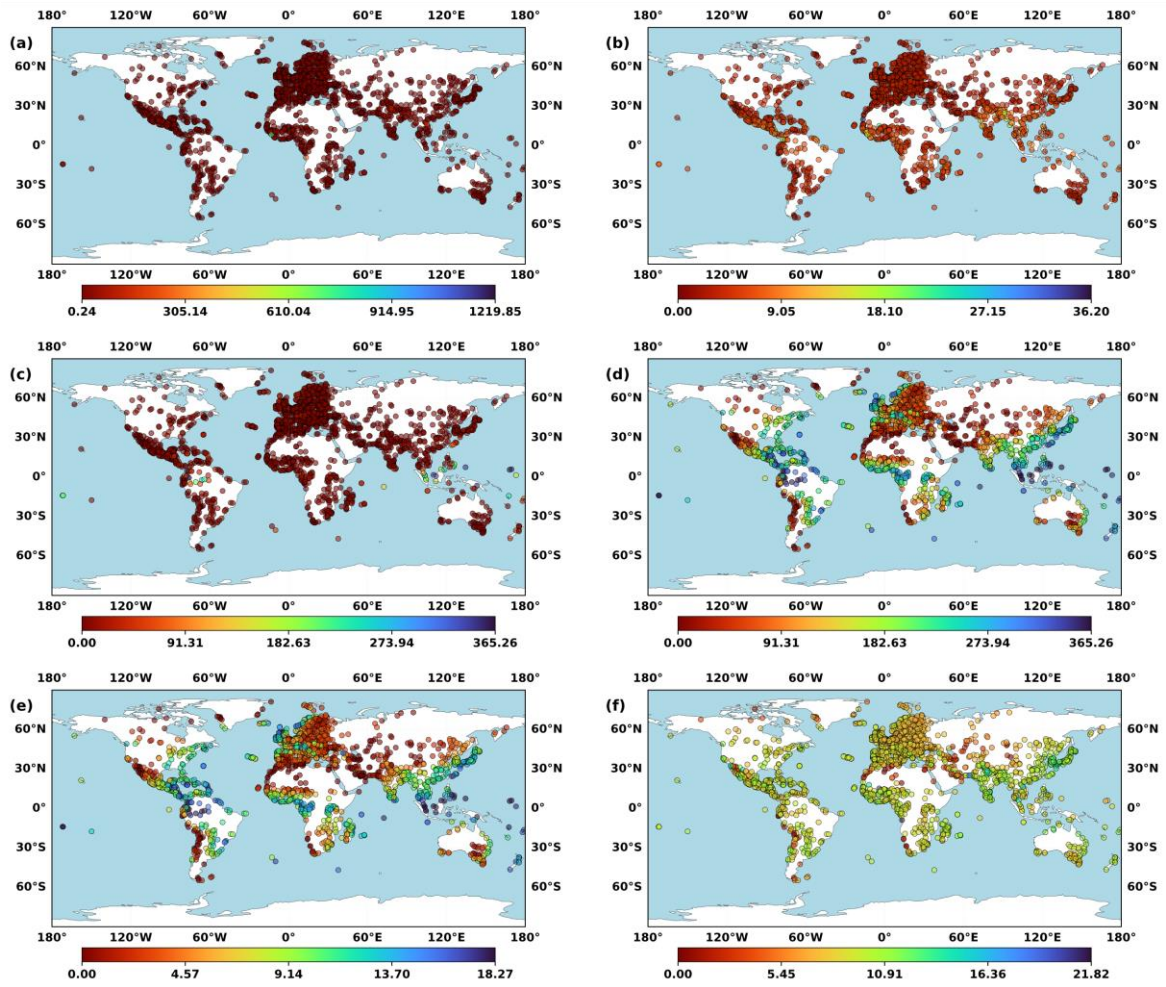

Figure 14: Geographical patterns of precipitation extremes indices in global wetlands during the historical SSP 585 scenario (1951 - 2024).

Rx1 exceeds 130 mm within specific parts of Asia, including the western coastal belt of Southern America, highlighted in deep red (a), while SDII reaches up to 20 mm/day across Africa and Asia, shown in purple (b). CWD exceeds 60 days in Europe and South America (c), marked in dark violet, and RD surpasses 300 days in Central Africa and Southeast Asia, indicated by dark red (d). RR95 occurs more than 28 times annually in Asia and South America (e), with red and yellow shades, while R95pTOT exceeds 35% in Central Africa and the Amazon Basin, represented in brown (f). Under the SSP 585 historical scenario (1951 - 2024) shown in Figure 14, wetlands across all global regions already exhibit strong signatures of hydrological stress driven by precipitation extremes. The most intense rainfall characteristics are concentrated in Asia, South America, and the Global Tropics, where Rx1 ranges from 90 - 140 mm, and SDII reaches 9 - 12 mm/day, indicating frequent and forceful rainfall bursts.

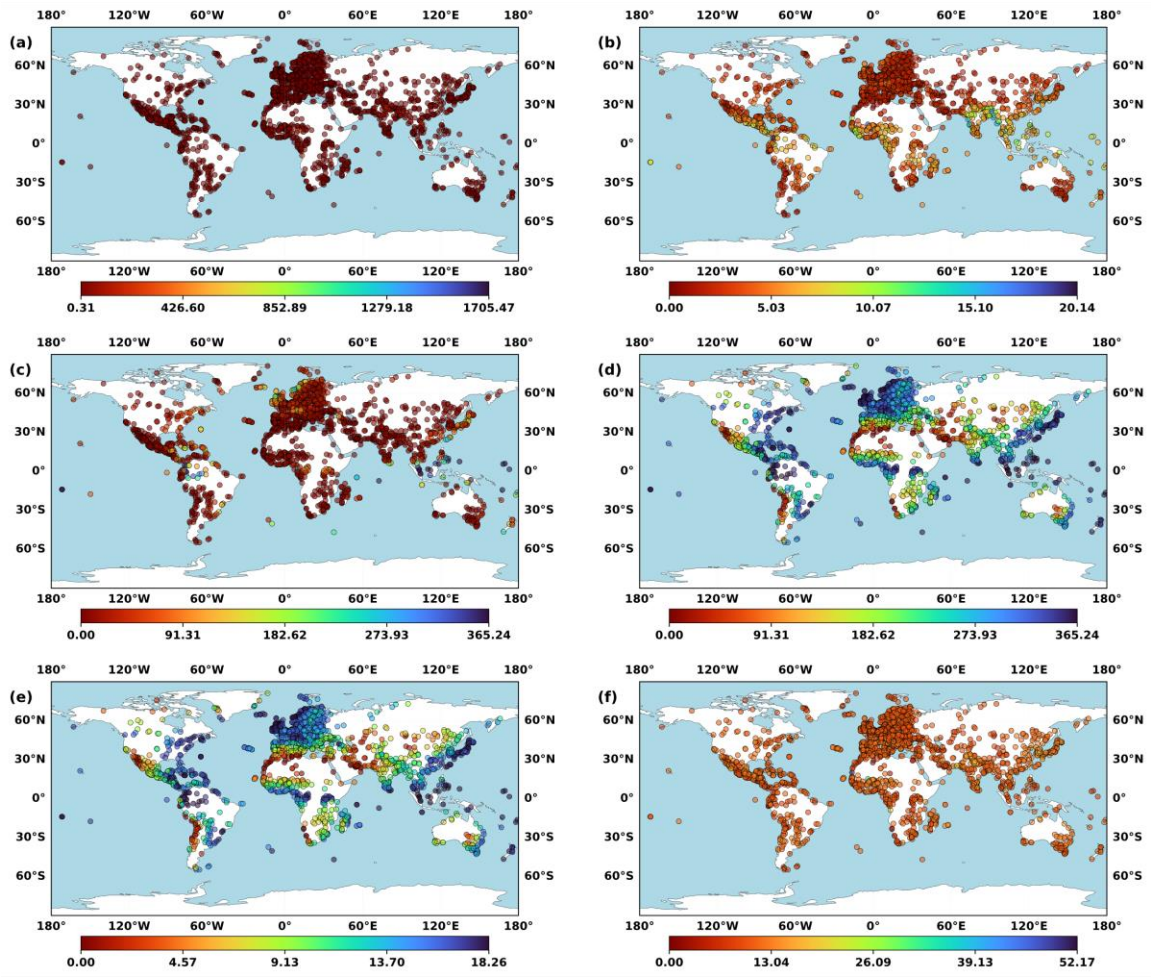

Figure 15: Geographical patterns of precipitation extremes indices in global wetlands during the future SSP 585 scenario (2025 - 2100).

These regions also experience CWD extending up to 45 days, while RR95 occurs 14 - 26 times annually, contributing as much as 35% of R95pTOT - a sign of highly clustered and flood-prone rainfall regimes. In contrast, Europe and Oceania display more moderate extremes, with Rx1 between 70 - 105 mm, SDII between 6 - 9 mm/day, and R95pTOT remaining below 20%, suggesting a relatively stable but less intense precipitation structure. However, even these regions are not exempt from pressure, as wet spell durations exceed 40 days, and RD still reaches 130 - 160 days, indicating evolving seasonal imbalances. Africa and North America fall in the middle of this spectrum, marked by a dual burden of extremes: SDII up to 12 mm/day and RR95 up to 24 events/year, combined with extended dry spells of 160 - 180 days, especially in sub-Saharan and southwestern areas.

These findings confirm that even under historical climate forcing, a significant proportion of global wetlands are already experiencing rainfall regimes characterized by high

intensity, prolonged wet or dry phases, and increasing dependence on a small number of extreme events, all of which heighten the risk of waterlogging, drought, and ecological disruption in these sensitive ecosystems.

Rx1 ranges from 0 to over 160 mm, with deep red shades marking the most intense events (a), (b) SDII, (c) CWD (range), (d) RD, (e) RR95 occur more than 30 times annually, and f) the percentage of rainfall contributed by R95pTOT exceeds 40% in many tropical sites. Under the SSP 585 future scenario (2025 - 2100) shown in Figure 15, Global projections indicate that nearly all regions will face heightened precipitation extremes, with the most significant changes expected in the Global Tropics, Asia, along with South America, emerging as the most impacted zones. Rx1 reaches 130 - 170 mm in the tropics, compared to 120 - 160 mm in Asia and South America, and around 80 - 120 mm in Europe. Similarly, SDII exceeds 14 mm/day in Africa and the tropics, highlighting a steep rise in event-scale intensity relative to more modest increases of 8 - 11 mm/day in temperate zones. In terms of temporal patterns, CWD is projected to extend beyond 50 days in the tropics and Europe. RD remains longest in Africa and Oceania, reaching up to 180 days, reflecting an intensification of seasonal rainfall imbalance. The RR95 also shows a notable rise, with the tropics and South America experiencing 20 - 34 events/year, compared to 12 - 22 events/year in Europe and Oceania. Crucially, the share of annual precipitation contributed by R95pTOT exceeds 40% in the tropics, 35% in Asia and South America, and reaches 30% even in North America, demonstrating a global shift toward rainfall clustering. Collectively, these trends suggest that Asia, South America, and Africa face the most severe intensification across all metrics, while Europe, North America, and Oceania also exhibit significant changes, especially in the form of longer wet spells and increased rainfall concentration, demonstrating a widespread global escalation in wetland hydrological extremes.

6. Conclusion

This global assessment of 2,490 Ramsar wetlands demonstrates that climate change is driving substantial and regionally concentrated shifts in precipitation variability, with the most pronounced impacts in Africa and Asia. These continents consistently have the highest numbers of wetlands transitioning into higher variability categories, particularly from low or medium to high and very high, highlighting increasing hydrological instability and ecological vulnerability. On a monthly scale, Africa dominates the very high variability category, especially in February, when 66 out of 74 very high variability sites globally are located on the continent, and Asia accounts for the remainder. Notably, some African sites, such as Nguru Lake and the Marma Channel Complex, move from low to high variability, reflecting a rare and significant reclassification. Similarly, Isla San Pedro Mártir in North America shifts from low to medium variability, indicating a substantial change in its internal dynamics. These upgrades in variability class signal heightened sensitivity to climatic fluctuations and the potential for ecological disruption. Conversely, several sites experience abrupt downgrades in variability. As Zarivar in Asia moves from medium to low variability and Île Blanche in Africa drops from high to low variability, both reflect a marked loss of hydrological complexity.

Particularly concerning are sites that transition directly from very high to low variability within a single period, as observed in two African sites (December) and one Asian site (January), which may indicate regime shifts or ecological thresholds being crossed. Directional analysis of category transitions further underscores the dynamic nature of these changes: under SSP245, 100 sites moved to higher variability categories, while 109 shifted downward; under SSP585, 117 upgrades, and 120 downgrades were recorded. Such bidirectional movements highlight the fluidity and unpredictability of wetland responses to climate forcing, with Africa and Asia showing the greatest volatility. While most wetlands remain in the low variability category, the widespread and sometimes dramatic internal entropy changes within these classes—such as the notable increases at Maladumba Lake (Nigeria) and East Calcutta Wetlands (India) demonstrate that apparent class stability can mask significant internal dynamism and emerging risks. In summary, under both moderate and high-emission scenarios, Ramsar wetlands, especially those in Africa and Asia, are increasingly at risk of shifting into higher variability categories, with some sites experiencing rare and substantial category conversions. These trends represent a serious

situation for wetland resilience, ecosystem services, and biodiversity, underscoring the urgent need for region-specific monitoring, adaptive management, and targeted conservation strategies to address the accelerating impacts of climate change on the world's most vulnerable wetland landscapes.

In the historical SSP 245 scenario, precipitation extremes remain moderate, with most wetlands recording PRCPTOT values between 600 - 1000 mm and most sites falling in the 20 - 40 days range for R10 and 11 - 20 days for R20. Rx1 values are largely below 40 mm. Indices R95pTOT and R99pTOT predominantly fall within the lower ranges, remaining between 0–5% and 0–2%, respectively. During the historical baseline under the SSP 585 pathway, similar patterns are observed with slight intensification; more wetlands cross into the 1000 - 1200 mm PRCPTOT range, R10 increases into the 41 - 60 days class, and R20 shifts into 21 - 40 days. Likewise, Rx1 shows a small increase with more wetlands exceeding 40 mm, and R95pTOT expands into the 5 - 10% category in some regions. Future projections under SSP 245 indicate a clear intensification of extremes. PRCPTOT increases, with many wetlands shifting into the 1000 - 1500 mm class. R10 predominantly increases to 41 - 60 days, and R20 moves further into 21 - 40 days. Rx1 surpasses 60 mm in several wetlands. Likewise, R95pTOT rises into the 10 - 15% range, and R99pTOT shows increases into 5 - 6% for specific wetlands. The future SSP 585 scenario shows the strongest intensification across nearly all indices. PRCPTOT values markedly increase, with large wetland regions exceeding 1500 - 2000 mm and many surpassing 2000 - 3000 mm. R10 exceeds 60 days, and R20 reaches 40 - 60 days in a wide area. Short-duration extremes intensify notably, with Rx1 values surpassing 80 mm and Rx5 crossing 200 mm, with some wetlands reaching >300 mm. R95pTOT peaks beyond 15 - 20%, and R99pTOT rises above 8 - 10% across multiple regions. Similarly, RR95 increases from 0 - 5 days historically to 10 - 15 days under SSP 585, while RR99 grows from 0 - 1 day to 2 - 3 days. CWD shows more modest increases, shifting from 5 - 10 days historically to 16 - 20 days in several regions under SSP 585. Overall, the spatial extent of wetlands exposed to extreme precipitation intensities expands substantially under SSP 585, with several indices (e.g., PRCPTOT >2000 mm) showing classes not reached under historical or SSP 245 scenarios.

Differences: SSP 245 Historical vs SSP 585 Historical

Under SSP 585 historical conditions, Rx1 values (max 1-day rainfall) are slightly higher, exceeding 130 mm in more locations (e.g., Asia, South America) compared to SSP 245,

where values mostly remain below 130 mm. Similarly, SDII reaches up to 20 mm/day more frequently in SSP 585, especially across Africa and South Asia, indicating higher storm intensity. CWD extends beyond 60 days more widely in SSP 585, particularly in Europe and South America, while SSP 245 shows this only in fewer pockets. It suggests longer periods of sustained rainfall under SSP 585. RD is slightly elevated in SSP 585 in Central Africa and Southeast Asia, with more wetlands exceeding 300 rainy days/year. SSP 245 also shows high RD but with slightly less spatial spread in extreme zones. SSP 585 exhibits more sites with RR95 > 25 days/year, particularly in South America, Asia, and Africa, compared to SSP 245. It implies that very wet days are more frequent in SSP 585, even under historical conditions. The contribution of total precipitation (R95pTOT) is considerably higher under SSP 585, with more wetlands crossing the 35 - 40% threshold, especially in the Amazon, Congo Basin, and parts of Asia. It signals a stronger rainfall concentration in SSP 585.

Difference between SSP 245 Future vs SSP 585 Future

In SSP 585, Rx1 values exceed 160 mm in several regions, such as Asia and South America, whereas most values fall below 140 - 150 mm in SSP 245. It indicates sharper rainfall bursts under SSP 585, reflecting the influence of stronger radiative forcing. SDII reaches more than 20 mm/day in SSP 585, especially in Africa and Southeast Asia, while SSP 245 stays mostly below 18 mm/day. Future conditions modeled by SSP 585 suggest that heavy rainfall will become more pronounced. Such heightened precipitation intensity could potentially cause disruptions to ecosystems or result in habitat loss, particularly affecting wetland species that are vulnerable to heavy rainfall. SSP 585 shows more wetlands with CWD > 60 days, especially in Europe and northern latitudes, compared to SSP 245, where such long wet periods are less widespread. This implies longer, uninterrupted wet phases under higher emissions. While both scenarios show RD > 300 days/year in the equatorial zone, SSP 585 has broader coverage, indicating more persistent annual rainfall in regions like Central Africa and Southeast Asia. Under SSP 585, RR95 exceeds 30 days/year in many tropical wetlands, more than in SSP 245, where RR95 is mostly under 28. This means that extreme wet days become more frequent under SSP 585. SSP 585 intensifies rainfall clustering, with R95pTOT > 40% in many areas (especially Amazon, Congo Basin, and South Asia), compared to SSP 245, where values generally remain under 35%. It reflects a greater reliance on extreme days for annual rainfall under higher forcing.

Building on the integrated entropy and climate extremes framework applied to global Ramsar wetlands, several promising avenues for future research emerge. First, expanding the analysis to incorporate additional hydroclimatic variables such as temperature extremes, evapotranspiration, and groundwater dynamics could provide a more holistic assessment of wetland vulnerability under climate change1. There is an opportunity to improve the spatial and temporal resolution of climate projections, enabling targeted adaptation strategies for wetlands in regions that are highly variable or lack sufficient data.

Further, coupling entropy-based metrics with ecological and socio-economic indicators would enhance our understanding of how changes in precipitation variability and extremes translate to impacts on wetland-dependent communities, biodiversity, and ecosystem services1. Long-term monitoring and the integration of remote sensing data can help validate model projections and detect early warning signals of regime shifts or ecological thresholds being crossed. Finally, future research should explore the effectiveness of adaptive management and restoration interventions in mitigating the identified risks, particularly in regions projected to experience the most dramatic shifts in variability and extremes. Collaborative, transboundary studies and the development of decision-support tools based on the presented methodology can inform international conservation policy and support the resilience of wetlands worldwide.

References

- Abraham, A., Kundapura, S., 2022. Evaluating the long-term trends of the climatic variables over three humid tropical basins in Kerala, India. Arab. J. Geosci. 15, 811. https://doi.org/10.1007/s12517-022-10056-y
- Afuye, G.A., Kalumba, A.M., Busayo, E.T., Orimoloye, I.R., 2022. A bibliometric review of vegetation response to climate change. Environ. Sci. Pollut. Res. 29, 18578–18590. https://doi.org/10.1007/s11356-021-16319-7
- Afuye, G.A., Kalumba, A.M., Owolabi, S.T., Thamaga, K.H., Ndou, N., Sibandze, P., Orimoloye, I.R., 2024. Analyzing spatiotemporal variations and dynamics of vegetation over Amathole district municipality in South Africa. Environ. Dev. Sustain. https://doi.org/10.1007/s10668-024-05221-0
- Aguirre-Liguori, J.A., Ramírez-Barahona, S., Gaut, B.S., 2021. The evolutionary genomics of species' responses to climate change. Nat. Ecol. Evol. 5, 1350–1360. https://doi.org/10.1038/s41559-021-01526-9
- Åhlén, I., Thorslund, J., Hambäck, P., Destouni, G., Jarsjö, J., 2022. Wetland position in the landscape: Impact on water storage and flood buffering. Ecohydrology 15, e2458. https://doi.org/https://doi.org/10.1002/eco.2458
- Alaminie, A.A., Amarnath, G., Padhee, S.K., Ghosh, S., Tilahun, S.A., Mekonnen, M.A., Assefa, G., Seid, A., Zimale, F.A., Jury, M.R., 2023. Nested hydrological modeling for flood prediction using CMIP6 inputs around Lake Tana, Ethiopia. J. Hydrol. Reg. Stud. 46, 101343. https://doi.org/10.1016/j.ejrh.2023.101343
- Alemayehu, A., Maru, M., Bewket, W., Assen, M., 2020. Spatiotemporal variability and trends in rainfall and temperature in Alwero watershed, western Ethiopia. Environ. Syst. Res. 9, 22. https://doi.org/10.1186/s40068-020-00184-3
- Alexander, L. V, Uotila, P., Nicholls, N., 2009. Influence of sea surface temperature variability on global temperature and precipitation extremes. J. Geophys. Res. Atmos. 114. https://doi.org/https://doi.org/10.1029/2009JD012301
- Almazroui, M., Saeed, F., Saeed, S., Ismail, M., Ehsan, M.A., Islam, M.N., Abid, M.A., O'Brien, E., Kamil, S., Rashid, I.U., Nadeem, I., 2021. Projected Changes in Climate Extremes Using CMIP6 Simulations Over SREX Regions. Earth Syst. Environ. 5, 481–497. https://doi.org/10.1007/s41748-021-00250-5
- AlSubih, M., Kumari, M., Mallick, J., Ramakrishnan, R., Islam, S., Singh, C.K., 2021. Time series trend analysis of rainfall in last five decades and its quantification in Aseer Region of Saudi Arabia. Arab. J. Geosci. 14, 519. https://doi.org/10.1007/s12517-021-06935-5
- Anand, V., Oinam, B., Wieprecht, S., 2024. Synergistic impact of climate and land use land cover change dynamics on the hydrological regime of Loktak Lake catchment under CMIP6 scenarios. J. Hydrol. Reg. Stud. 53, 101851. https://doi.org/10.1016/j.ejrh.2024.101851
- Avila-Diaz, A., Abrahão, G., Justino, F., Torres, R., Wilson, A., 2020. Extreme climate indices in Brazil: evaluation of downscaled earth system models at high horizontal resolution. Clim. Dyn. 54, 5065–5088. https://doi.org/10.1007/s00382-020-05272-9
- Baig, M.R.I., Shahfahad, Naikoo, M.W., Ansari, A.H., Ahmad, S., Rahman, A., 2022. Spatio-temporal analysis of precipitation pattern and trend using standardized precipitation index and Mann–Kendall test in coastal Andhra Pradesh. Model. Earth Syst. Environ. 8, 2733–2752. https://doi.org/10.1007/s40808-021-01262-w

- Baker, J., Dupont, D., Vasseur, L., 2021. Exploring Canadian Ramsar Sites Ecosystem Governance and Sustainability. Wetlands 41, 6. https://doi.org/10.1007/s13157-021-01417-6
- Balzter, H., Tate, N., Kaduk, J., Harper, D., Page, S., Morrison, R., Muskulus, M., Jones, P., 2015. Multi-Scale Entropy Analysis as a Method for Time-Series Analysis of Climate Data. Climate 3, 227–240. https://doi.org/10.3390/cli3010227
- Bandt, C., Pompe, B., 2002. Permutation Entropy: A Natural Complexity Measure for Time Series. Phys. Rev. Lett. 88, 174102. https://doi.org/10.1103/PhysRevLett.88.174102
- Bastos, A., Sippel, S., Frank, D., Mahecha, M.D., Zaehle, S., Zscheischler, J., Reichstein, M., 2023. A joint framework for studying compound ecoclimatic events. Nat. Rev. Earth Environ. 4, 333–350. https://doi.org/10.1038/s43017-023-00410-3
- Bayat, B., Nasseri, M., Hosseini, K., Karami, H., 2021. Nested Augmentation of Rainfall Monitoring Network: Proposing a Hybrid Implementation of Block Kriging and Entropy Theory. Water Resour. Manag. 35, 4665–4680. https://doi.org/10.1007/s11269-021-02976-3
- Bayazit, M., 2015. Nonstationarity of Hydrological Records and Recent Trends in Trend Analysis: A State-of-the-art Review. Environ. Process. 2, 527–542. https://doi.org/10.1007/s40710-015-0081-7
- Beck, H.E., McVicar, T.R., Vergopolan, N., Berg, A., Lutsko, N.J., Dufour, A., Zeng, Z., Jiang, X., van Dijk, A.I.J.M., Miralles, D.G., 2023. High-resolution (1 km) Köppen-Geiger maps for 1901–2099 based on constrained CMIP6 projections. Sci. Data 10, 724. https://doi.org/10.1038/s41597-023-02549-6
- Beck, H.E., Zimmermann, N.E., McVicar, T.R., Vergopolan, N., Berg, A., Wood, E.F., 2020. Publisher Correction: Present and future Köppen-Geiger climate classification maps at 1-km resolution. Sci. Data 7, 274. https://doi.org/10.1038/s41597-020-00616-w
- Becker, M., Seeger, K., Paszkowski, A., Marcos, M., Papa, F., Almar, R., Bates, P., France-Lanord, C., Hossain, M.S., Khan, M.J.U., Karegar, M.A., Karpytchev, M., Long, N., Minderhoud, P.S.J., Neal, J., Nicholls, R.J., Syvitski, J., 2024. Coastal Flooding in Asian Megadeltas: Recent Advances, Persistent Challenges, and Call for Actions Amidst Local and Global Changes. Rev. Geophys. 62, e2024RG000846. https://doi.org/https://doi.org/10.1029/2024RG000846
- Birnbaum, C., Waryszak, P., Farrer, E.C., 2021. Direct and Indirect Effects of Climate Change in Coastal Wetlands: Will Climate Change Influence Wetlands by Affecting Plant Invasion? Wetlands 41, 59. https://doi.org/10.1007/s13157-021-01456-z
- Bobde, V., Akinsanola, A.A., Folorunsho, A.H., Adebiyi, A.A., Adeyeri, O.E., 2024. Projected regional changes in mean and extreme precipitation over Africa in CMIP6 models. Environ. Res. Lett. 19, 074009. https://doi.org/10.1088/1748-9326/ad545c
- Brunsell, N.A., 2010. A multiscale information theory approach to assess spatial–temporal variability of daily precipitation. J. Hydrol. 385, 165–172. https://doi.org/https://doi.org/10.1016/j.jhydrol.2010.02.016
- Butterfield, B.J., Palmquist, E.C., 2023. Inundation Tolerance, Rather than Drought Tolerance, Predicts Riparian Plant Distributions Along a Local Hydrologic Gradient. Wetlands 44, 6. https://doi.org/10.1007/s13157-023-01730-2
- Chan, F.K.S., Paszkowski, A., Wang, Z., Lu, X., Mitchell, G., Tran, D.D., Warner,

J., Li, J., Chen, Y.D., Li, N., Pal, I., Griffiths, J., Chen, J., Chen, W.-Q., Zhu, Y.-G., 2024. Building resilience in Asian mega-deltas. Nat. Rev. Earth Environ. 5, 522–537. https://doi.org/10.1038/s43017-024-00561-x

- Chang, M., Liu, B., Wang, B., Martinez-Villalobos, C., Ren, G., Zhou, T., 2022. Understanding Future Increases in Precipitation Extremes in Global Land Monsoon Regions. J. Clim. 35, 1839–1851. https://doi.org/10.1175/JCLI-D-21-0409.1
- Chapagain, D., Dhaubanjar, S., Bharati, L., 2021. Unpacking future climate extremes and their sectoral implications in western Nepal. Clim. Change 168, 8. https://doi.org/10.1007/s10584-021-03216-8
- Cheng, L., Niu, J., Liao, D., 2017. Entropy-Based Investigation on the Precipitation Variability over the Hexi Corridor in China. Entropy 19, 660. https://doi.org/10.3390/e19120660
- Chervenkov, H., Slavov, K., 2021. ETCCDI Climate Indices for Assessment of the Recent Climate over Southeast Europe, in: Dimov, I., Fidanova, S. (Eds.), Advances in High Performance Computing. Springer International Publishing, Cham, pp. 398–412.
- Chetan Kumar, S., Syam N, S.S., Rathinasamy, M., 2024. Assessment of spatial variability of precipitation in Krishna River Basin using a metric based on apportionment entropy. Hydrol. Sci. J. 1–15. https://doi.org/10.1080/02626667.2024.2376708
- Choobeh, S., Abghari, H., Erfanian, M., 2024. Spatial and temporal variability of precipitation based on marginal and apportionment entropy disorder indices in Iran. Theor. Appl. Climatol. 155, 2589–2603. https://doi.org/10.1007/s00704-023-04748-y
- Darbandsari, P., Coulibaly, P., 2022. Assessing Entropy-Based Bayesian Model Averaging Method for Probabilistic Precipitation Forecasting. J. Hydrometeorol. 23, 421–440. https://doi.org/10.1175/JHM-D-21-0086.1
- Davidson, N.C., 2014. How much wetland has the world lost? Long-term and recent trends in global wetland area. Mar. Freshw. Res. 65, 934–941. https://doi.org/10.1071/MF14173
- Dawson, B., Spannagle, M., 2020. Intergovernmental Panel on Climate Change (Ipcc), The Complete Guide to Climate Change. https://doi.org/10.4324/9780203888469-41
- Day, J., Anthony, E., Costanza, R., Edmonds, D., Gunn, J., Hopkinson, C., Mann, M.E., Morris, J., Osland, M., Quirk, T., Rovai, A., Rybczyk, J., Spencer, T., Stephens, J., Syvitski, J., Twilley, R., Visser, J., White, J.R., 2024. Coastal Wetlands in the Anthropocene. Annu. Rev. Environ. Resour. 49, 105–135. https://doi.org/10.1146/annurev-environ-121922-041109
- de P. Rodrigues da Silva, V., Belo Filho, A.F., Rodrigues Almeida, R.S., de Holanda, R.M., da Cunha Campos, J.H.B., 2016. Shannon information entropy for assessing space–time variability of rainfall and streamflow in semiarid region. Sci. Total Environ. 544, 330–338. https://doi.org/https://doi.org/10.1016/j.scitotenv.2015.11.082
- de Vries, I., Sippel, S., Zeder, J., Fischer, E., Knutti, R., 2024. Increasing extreme precipitation variability plays a key role in future record-shattering event probability. Commun. Earth Environ. 5, 482. https://doi.org/10.1038/s43247-024-01622-1
- Deepa, R., Kumar, V., Sundaram, S., 2024. A systematic review of regional and global climate extremes in CMIP6 models under shared socio-economic pathways.

Theor. Appl. Climatol. 155, 2523–2543. https://doi.org/10.1007/s00704-024-04872-3
- Dittus, A.J., Karoly, D.J., Donat, M.G., Lewis, S.C., Alexander, L. V, 2018. Understanding the role of sea surface temperature-forcing for variability in global temperature and precipitation extremes. Weather Clim. Extrem. 21, 1–9. https://doi.org/https://doi.org/10.1016/j.wace.2018.06.002
- Donat, M.G., Alexander, L. V., Herold, N., Dittus, A.J., 2016. Temperature and precipitation extremes in century-long gridded observations, reanalyses, and atmospheric model simulations. J. Geophys. Res. Atmos. 121. https://doi.org/10.1002/2016JD025480
- Dong, T., Dong, W., 2021. Evaluation of extreme precipitation over Asia in CMIP6 models. Clim. Dyn. 57, 1751–1769. https://doi.org/10.1007/s00382-021-05773-1
- Du, L., Li, X., Yang, M., Sivakumar, B., Zhu, Y., Pan, X., Li, Z., Sang, Y.-F., 2022. Assessment of spatiotemporal variability of precipitation using entropy indexes: a case study of Beijing, China. Stoch. Environ. Res. Risk Assess. 36, 939–953. https://doi.org/10.1007/s00477-021-02116-8
- Duchenne-Moutien, R.A., Neetoo, H., 2021. Climate Change and Emerging Food Safety Issues: A Review. J. Food Prot. 84, 1884–1897. https://doi.org/https://doi.org/10.4315/JFP-21-141
- Eekhout, J.P.C., Hunink, J.E., Terink, W., de Vente, J., 2018. Why increased extreme precipitation under climate change negatively affects water security. Hydrol. Earth Syst. Sci. 22, 5935–5946. https://doi.org/10.5194/hess-22-5935-2018
- Elgendy, M., Hassini, S., Coulibaly, P., 2024. Review of Climate Change Adaptation Strategies in Water Management. J. Hydrol. Eng. 29. https://doi.org/10.1061/JHYEFF.HEENG-6014
- Erwin, K.L., 2009. Wetlands and global climate change: the role of wetland restoration in a changing world. Wetl. Ecol. Manag. 17, 71–84. https://doi.org/10.1007/s11273-008-9119-1
- Eyring, V., Bony, S., Meehl, G.A., Senior, C., Stevens, B., Stouffer, R.J., Taylor, K.E., 2015. Overview of the Coupled Model Intercomparison Project Phase 6 (CMIP6) experimental design and organisation. https://doi.org/10.5194/gmdd-8-10539-2015
- Eyring, V., Bony, S., Meehl, G.A., Senior, C.A., Stevens, B., Stouffer, R.J., Taylor, K.E., 2016. Overview of the Coupled Model Intercomparison Project Phase 6 (CMIP6) experimental design and organization. Geosci. Model Dev. 9, 1937–1958. https://doi.org/10.5194/gmd-9-1937-2016
- Feng, X., Porporato, A., Rodriguez-Iturbe, I., 2013. Changes in rainfall seasonality in the tropics. Nat. Clim. Chang. 3, 811–815. https://doi.org/10.1038/nclimate1907
- Fluet-Chouinard, E., Stocker, B.D., Zhang, Z., Malhotra, A., Melton, J.R., Poulter, B., Kaplan, J.O., Goldewijk, K.K., Siebert, S., Minayeva, T., Hugelius, G., Joosten, H., Barthelmes, A., Prigent, C., Aires, F., Hoyt, A.M., Davidson, N., Finlayson, C.M., Lehner, B., Jackson, R.B., McIntyre, P.B., 2023. Extensive global wetland loss over the past three centuries. Nature 614, 281–286. https://doi.org/10.1038/s41586-022-05572-6
- Gehlot, L.K., Jibhakate, S.M., Sharma, P.J., Patel, P.L., Timbadiya, P. V., 2021. Spatio-Temporal Variability of Rainfall Indices and their Teleconnections with El Niño-Southern Oscillation for Tapi Basin, India. Asia-Pacific J. Atmos. Sci. 57, 99–118. https://doi.org/10.1007/s13143-020-00179-1
- Geijzendorffer, I.R., Beltrame, C., Chazee, L., Gaget, E., Galewski, T., Guelmami,

A., Perennou, C., Popoff, N., Guerra, C.A., Leberger, R., Jalbert, J., Grillas, P., 2019. A More Effective Ramsar Convention for the Conservation of Mediterranean Wetlands. Front. Ecol. Evol. 7. https://doi.org/10.3389/fevo.2019.00021

- Ghorbani, M.A., Kahya, E., Roshni, T., Kashani, M.H., Malik, A., Heddam, S., 2021. Entropy analysis and pattern recognition in rainfall data, north Algeria. Theor. Appl. Climatol. 144, 317–326. https://doi.org/10.1007/s00704-021-03542-y
- Goffin, B.D., Kansara, P., Lakshmi, V., 2024. Intensification in the Wettest Days to 50 Percent of Annual Precipitation (WD50) Across Europe. Geophys. Res. Lett. 51, e2023GL107403. https://doi.org/https://doi.org/10.1029/2023GL107403
- Golden, H.E., Lane, C.R., Adnan, R., Qiusheng, W., 2021. Improving global flood and drought predictions: integrating non-floodplain wetlands into watershed hydrologic models. Environ. Res. Lett. 16, 1–5. https://doi.org/10.1088/1748-9326/ac1fbc
- Goyal, M.K., Gupta, A.K., Das, J., Jain, V., Rakkasagi, S., 2023a. Heatwave magnitude impact over Indian cities: CMIP 6 projections. Theor. Appl. Climatol. 154, 959–971. https://doi.org/10.1007/s00704-023-04599-7
- Goyal, M.K., Gupta, A.K., Jha, S., Rakkasagi, S., Jain, V., 2022. Climate change impact on precipitation extremes over Indian cities: Non-stationary analysis. Technol. Forecast. Soc. Change 180, 121685. https://doi.org/10.1016/j.techfore.2022.121685
- Goyal, M.K., Rakkasagi, S., Shaga, S., Zhang, T.C., Surampalli, R.Y., Dubey, S., 2023b. Spatiotemporal-based automated inundation mapping of Ramsar wetlands using Google Earth Engine. Sci. Rep. 13, 17324. https://doi.org/10.1038/s41598-023-43910-4
- Goyal, M.K., Rakkasagi, S., Surampalli, R.Y., Zhang, T.C., Erumalla, S., Gupta, A., Dubey, S., U-tapao, C., 2024. Enhancing sustainable development through Spatiotemporal analysis of Ramsar wetland sites in South Asia. Technol. Soc. 79, 102723. https://doi.org/https://doi.org/10.1016/j.techsoc.2024.102723
- Goyette, J.-O., Savary, S., Blanchette, M., Rousseau, A.N., Pellerin, S., Poulin, M., 2023. Setting Targets for Wetland Restoration to Mitigate Climate Change Effects on Watershed Hydrology. Environ. Manage. 71, 365–378. https://doi.org/10.1007/s00267-022-01763-z
- Granata, F., Di Nunno, F., 2025. Pathways for Hydrological Resilience: Strategies for Adaptation in a Changing Climate. Earth Syst. Environ. https://doi.org/10.1007/s41748-024-00567-x
- Grieger, R., Capon, S.J., Hadwen, W.L., Mackey, B., 2020. Between a bog and a hard place: a global review of climate change effects on coastal freshwater wetlands. Clim. Change 163, 161–179. https://doi.org/10.1007/s10584-020-02815-1
- Guntu, R. kumar, Agarwal, A., 2020. Standardized Variability Index (SVI) : A multiscale index to assess the variability of precipitation. 2nd JPGU-AGU 2020 7–12. https://doi.org/10.1002/essoar.10503941.1
- Guntu, R.K., Maheswaran, R., Agarwal, A., Singh, V.P., 2020a. Accounting for temporal variability for improved precipitation regionalization based on self-organizing map coupled with information theory. J. Hydrol. 590, 125236. https://doi.org/10.1016/j.jhydrol.2020.125236
- Guntu, R.K., Rathinasamy, M., Agarwal, A., Sivakumar, B., 2020b. Spatiotemporal variability of Indian rainfall using multiscale entropy. J. Hydrol. 587, 124916. https://doi.org/10.1016/j.jhydrol.2020.124916

- Gupta, V., Rakkasagi, S., Rajpoot, S., Imanni, H.S. El, Singh, S., 2023. Spatiotemporal analysis of Imja Lake to estimate the downstream flood hazard using the SHIVEK approach. Acta Geophys. 71, 2233–2244. https://doi.org/10.1007/s11600-023-01124-2
- Hardouin, L., Decharme, B., Colin, J., Delire, C., 2024. Climate-Driven Projections of Future Global Wetlands Extent. Earth's Futur. 12. https://doi.org/10.1029/2024EF004553
- Hassanlu, A., Erfanian, M., Javan, K., Najafi, M., 2023. Daily precipitation concentration and Shannon's entropy characteristics: spatial and temporal variability in Iran, 1966–2018. Theor. Appl. Climatol. 155, 1–23. https://doi.org/10.1007/s00704-023-04647-2
- Hempattarasuwan, N., Untong, A., Christakos, G., Wu, J., 2021. Wetland changes and their impacts on livelihoods in Chiang Saen Valley, Chiang Rai Province, Thailand. Reg. Environ. Chang. 21, 115. https://doi.org/10.1007/s10113-021-01842-7
- Hjort, J., Streletskiy, D., Doré, G., Wu, Q., Bjella, K., Luoto, M., 2022. Impacts of permafrost degradation on infrastructure. Nat. Rev. Earth Environ. 3, 24–38. https://doi.org/10.1038/s43017-021-00247-8
- Hobeichi, S., Abramowitz, G., Sen Gupta, A., Taschetto, A.S., Richardson, D., Rampal, N., Ayat, H., Alexander, L. V., Pitman, A.J., 2024. How well do climate modes explain precipitation variability? npj Clim. Atmos. Sci. 7, 295. https://doi.org/10.1038/s41612-024-00853-5
- Hu, Z., Chen, X., Chen, D., Li, J., Wang, S., Zhou, Q., Yin, G., Guo, M., 2019. "Dry gets drier, wet gets wetter": A case study over the arid regions of central Asia. Int. J. Climatol. 39, 1072–1091. https://doi.org/10.1002/joc.5863
- Hussain, S., Sharma, S., Bhatti, R.C., Singh, A.N., 2024. Sustainability in the Indian Himalayan Region: Understandings the Ecosystem Services, Climate Change Impacts, Land Use Shifts and Their Threats, in: Borthakur, A., Singh, P. (Eds.), The Himalayas in the Anthropocene: Environment and Development. Springer Nature Switzerland, Cham, pp. 33–57. https://doi.org/10.1007/978-3-031-50101-2_2
- Imdad, K., Sahana, M., Gautam, O., Chaudhary, A., Misra, S., Dwivedi, S., Ahmed, R., 2025. Anthropogenic and Hydroclimatic Drivers of Livelihood Vulnerability in Wetland Communities: A Geospatial and Pragmatic Assessment. Water Resour. Manag. 39, 2503–2525. https://doi.org/10.1007/s11269-024-04075-5
- IPCC, 2022. Global Warming of 1.5°C. Cambridge University Press. https://doi.org/10.1017/9781009157940
- IPCC, 2021. Climate Change 2021 The Physical Science Basis Working Group I Contribution to the Sixth Assessment Report of the Intergovernmental Panel on Climate Change.
- Jain, V., Kumar, S., Kumar Goyal, M., 2025. Relationship between daily precipitation extremes and temperature in changing climate across smart cities of Central India. J. Environ. Manage. 380, 125036. https://doi.org/10.1016/j.jenvman.2025.125036
- Jamion, N.A., Lee, K.E., Mokhtar, M., Goh, T.L., Simon, N., Goh, C.T., Bhat, I.U.H., 2023. The integration of nature values and services in the nature-based solution assessment framework of constructed wetlands for carbon–water nexus in carbon sequestration and water security. Environ. Geochem. Health 45, 1201–1230. https://doi.org/10.1007/s10653-022-01322-9
- Junk, W., An, S., Finlayson, M., Gopal, B., Květ, J., Mitchell, S., Mitsch, W.,

Robarts, R., 2013. Current state of knowledge regarding the world's wetlands and their future under global climate change: A synthesis. Aquat. Sci. 75. https://doi.org/10.1007/s00027-012-0278-z

- Kaboli, S., Hekmatzadeh, A.A., Darabi, H., Haghighi, A.T., 2021. Variation in physical characteristics of rainfall in Iran, determined using daily rainfall concentration index and monthly rainfall percentage index. Theor. Appl. Climatol. 144, 507–520. https://doi.org/10.1007/s00704-021-03553-9
- Karl, T.R., Nicholls, N., Ghazi, A., 1999. CLIVAR/GCOS/WMO Workshop on Indices and Indicators for Climate Extremes Workshop Summary, in: Weather and Climate Extremes. Springer Netherlands, Dordrecht, pp. 3–7. https://doi.org/10.1007/978-94-015-9265-9_2
- Kawachi, T., Maruyama, T., Singh, V.P., 2001. Rainfall entropy for delineation of water resources zones in Japan. J. Hydrol. 246, 36–44. https://doi.org/10.1016/S0022-1694 (01)00355-9
- Keum, J., Coulibaly, P., 2017. Information theory-based decision support system for integrated design of multivariable hydrometric networks. Water Resour. Res. 53, 6239–6259. https://doi.org/https://doi.org/10.1002/2016WR019981
- Kikstra, J.S., Nicholls, Z.R.J., Smith, C.J., Lewis, J., Lamboll, R.D., Byers, E., Sandstad, M., Meinshausen, M., Gidden, M.J., Rogelj, J., Kriegler, E., Peters, G.P., Fuglestvedt, J.S., Skeie, R.B., Samset, B.H., Wienpahl, L., van Vuuren, D.P., van der Wijst, K.-I., Al Khourdajie, A., Forster, P.M., Reisinger, A., Schaeffer, R., Riahi, K., 2022. The IPCC Sixth Assessment Report WGIII climate assessment of mitigation pathways: from emissions to global temperatures. Geosci. Model Dev. 15, 9075–9109. https://doi.org/10.5194/gmd-15-9075-2022
- Kim, Y.-H., Min, S.-K., Zhang, X., Sillmann, J., Sandstad, M., 2020. Evaluation of the CMIP6 multi-model ensemble for climate extreme indices. Weather Clim. Extrem. 29, 100269. https://doi.org/10.1016/j.wace.2020.100269
- Kingsford, R.T., Bino, G., Finlayson, C.M., Falster, D., Fitzsimons, J.A., Gawlik, D.E., Murray, N.J., Grillas, P., Gardner, R.C., Regan, T.J., Roux, D.J., Thomas, R.F., 2021. Ramsar Wetlands of International Importance–Improving Conservation Outcomes. Front. Environ. Sci. 9. https://doi.org/10.3389/fenvs.2021.643367
- Krstanovic, P.F., Singh, V.P., 1992. Evaluation of rainfall networks using entropy: I. Theoretical development. Water Resour. Manag. 6, 279–293. https://doi.org/10.1007/BF00872281
- Kuinkel, D., Promchote, P., Upreti, K.R., Wang, S.-Y.S., Dahal, N., Pokharel, B., 2024. Projected changes in precipitation extremes in Southern Thailand using CMIP6 models. Theor. Appl. Climatol. 155, 8703–8716. https://doi.org/10.1007/s00704-024-05150-y
- Kumar, A., Kumar, S., Rautela, K.S., Shekhar, S., Ray, T., Thangavel, M., 2023. Assessing seasonal variation and trends in rainfall patterns of Madhya Pradesh, Central India. J. Water Clim. Chang. 14, 3692–3712. https://doi.org/10.2166/wcc.2023.280
- Kumar, A., Thangavel, M., 2025. Unravelling the dynamics of rainfall patterns in Bihar, India: A comprehensive spatiotemporal analysis. Environ. Sci. Pollut. Res. 32, 8564–8584. https://doi.org/10.1007/s11356-025-36243-4
- Kundu, S., Kundu, B., Rana, N.K., Mahato, S., 2024. Wetland degradation and its impacts on livelihoods and sustainable development goals: An overview. Sustain. Prod. Consum. 48, 419–434. https://doi.org/https://doi.org/10.1016/j.spc.2024.05.024

- Lagos, P., Silva, Y., Nickl, E., Mosquera, K., 2008. El Niño – related precipitation variability in Perú. Adv. Geosci. 14, 231–237. https://doi.org/10.5194/adgeo-14-231-2008
- Lange, S., Büchner, M., 2020. ISIMIP2a atmospheric climate input data. https://doi.org/10.48364/ISIMIP.886955
- Lemus-Canovas, M., 2022. Changes in compound monthly precipitation and temperature extremes and their relationship with teleconnection patterns in the Mediterranean. J. Hydrol. 608, 127580. https://doi.org/https://doi.org/10.1016/j.jhydrol.2022.127580
- Li, Chao, Zwiers, F., Zhang, X., Li, G., Sun, Y., Wehner, M., 2021. Changes in Annual Extremes of Daily Temperature and Precipitation in CMIP6 Models. J. Clim. 34, 3441–3460. https://doi.org/10.1175/JCLI-D-19-1013.1
- Li, Hongwei, Li, Z., Chen, Y., Xiang, Y., Liu, Y., Kayumba, P.M., Li, X., 2021. Drylands face potential threat of robust drought in the CMIP6 SSPs scenarios. Environ. Res. Lett. 16, 114004. https://doi.org/10.1088/1748-9326/ac2bce
- Li, Heshu, Wang, D., Singh, V.P., Wang, Y., Wu, Jianfeng, Wu, Jichun, 2021. Developing an entropy and copula-based approach for precipitation monitoring network expansion. J. Hydrol. 598, 126366. https://doi.org/https://doi.org/10.1016/j.jhydrol.2021.126366
- Li, W., Guan, J., Wang, W., Wu, Y., Zhao, Y., Zhang, W., Wang, S., Chen, Z., 2024. Analysis of extreme precipitation variation characteristics in mountain grasslands of arid and semi-arid regions in China. Front. Environ. Sci. Volume 12. https://doi.org/10.3389/fenvs.2024.1403490
- Liaqat, W., Altaf, M.T., Barutçular, C., Nawaz, H., Ullah, I., Basit, A., Mohamed, H.I., 2024. Ultraviolet-B radiation in relation to agriculture in the context of climate change: a review. Cereal Res. Commun. 52, 1–24. https://doi.org/10.1007/s42976-023-00375-5
- Liu, X., Han, X., Han, Z., 2022. Effects of climate change on the potential habitat distribution of swimming crab Portunus trituberculatus under the species distribution model. J. Oceanol. Limnol. 40, 1556–1565. https://doi.org/10.1007/s00343-021-1082-1
- Lolu, A.J., Ahluwalia, A.S., Sidhu, M.C., Reshi, Z.A., Mandotra, S.K., 2020. Carbon Sequestration and Storage by Wetlands: Implications in the Climate Change Scenario, in: Upadhyay, A.K., Singh, R., Singh, D.P. (Eds.), Restoration of Wetland Ecosystem: A Trajectory Towards a Sustainable Environment. Springer Singapore, Singapore, pp. 45–58. https://doi.org/10.1007/978-981-13-7665-8_4
- Lovelock, C.E., Cahoon, D.R., Friess, D.A., Guntenspergen, G.R., Krauss, K.W., Reef, R., Rogers, K., Saunders, M.L., Sidik, F., Swales, A., Saintilan, N., Thuyen, L.X., Triet, T., 2015. The vulnerability of Indo-Pacific mangrove forests to sea-level rise. Nature 526, 559–563. https://doi.org/10.1038/nature15538
- Lu, H., Li, F., Gong, T., Gao, Y., Li, J., Wang, G., Qiu, J., 2022. Temporal variability of precipitation over the Qinghai-Tibetan Plateau and its surrounding areas in the last 40 years. Int. J. Climatol. 43. https://doi.org/10.1002/joc.7953
- Maharjan, M., Yoneda, M., Talchabhadel, R., Thapa, B.R., Aryal, A., 2023. Use of Indices on Daily Timescales to Study Changes in Extreme Precipitation Across Nepal Over 40 Years (1976–2015). Earth Sp. Sci. 10, e2020EA001509. https://doi.org/https://doi.org/10.1029/2020EA001509
- Maimone, M., Malter, S., Anbessie, T., Rockwell, J., 2023. Three methods of characterizing climate-induced changes in extreme rainfall: a comparison study. J.

Water Clim. Chang. 14, 4245–4260. https://doi.org/10.2166/wcc.2023.420
- Maruyama, T., Kawachi, T., Singh, V.P., 2005. Entropy-based assessment and clustering of potential water resources availability. J. Hydrol. 309, 104–113. https://doi.org/10.1016/j.jhydrol.2004.11.020
- Maurer, E.P., Hidalgo, H.G., 2007. Utility of daily vs. monthly large-scale climate data: an intercomparison of two statistical downscaling methods. https://doi.org/10.5194/hessd-4-3413-2007
- McDowell, N.G., Anderson-Teixeira, K., Biederman, J.A., Breshears, D.D., Fang, Y., Fernández-de-Uña, L., Graham, E.B., Mackay, D.S., McDonnell, J.J., Moore, G.W., Nehemy, M.F., Stevens Rumann, C.S., Stegen, J., Tague, N., Turner, M.G., Chen, X., 2023. Ecohydrological decoupling under changing disturbances and climate. One Earth 6, 251–266. https://doi.org/10.1016/j.oneear.2023.02.007
- Meinshausen, M., Nicholls, Z.R.J., Lewis, J., Gidden, M.J., Vogel, E., Freund, M., Beyerle, U., Gessner, C., Nauels, A., Bauer, N., Canadell, J.G., Daniel, J.S., John, A., Krummel, P.B., Luderer, G., Meinshausen, N., Montzka, S.A., Rayner, P.J., Reimann, S., Smith, S.J., van den Berg, M., Velders, G.J.M., Vollmer, M.K., Wang, R.H.J., 2020. The shared socio-economic pathway (SSP) greenhouse gas concentrations and their extensions to 2500. Geosci. Model Dev. 13, 3571–3605. https://doi.org/10.5194/gmd-13-3571-2020
- Meinshausen, M., Smith, S.J., Calvin, K., Daniel, J.S., Kainuma, M.L.T., Lamarque, J.-F., Matsumoto, K., Montzka, S.A., Raper, S.C.B., Riahi, K., Thomson, A., Velders, G.J.M., van Vuuren, D.P.P., 2011. The RCP greenhouse gas concentrations and their extensions from 1765 to 2300. Clim. Change 109, 213–241. https://doi.org/10.1007/s10584-011-0156-z
- Melnikov, A., Zhang, Z., Gagarin, L., 2024. Effects of extreme atmospheric precipitation on the stability of railways in the permafrost zone. Model. Earth Syst. Environ. 10, 1305–1320. https://doi.org/10.1007/s40808-023-01847-7
- Mishra, A.K., Özger, M., Singh, V.P., 2009. An entropy-based investigation into the variability of precipitation. J. Hydrol. 370, 139–154. https://doi.org/10.1016/j.jhydrol.2009.03.006
- Moi, D.A., Lansac-Tôha, F.M., Romero, G.Q., Sobral-Souza, T., Cardinale, B.J., Kratina, P., Perkins, D.M., Teixeira de Mello, F., Jeppesen, E., Heino, J., Lansac-Tôha, F.A., Velho, L.F.M., Mormul, R.P., 2022. Human pressure drives biodiversity–multifunctionality relationships in large Neotropical wetlands. Nat. Ecol. Evol. 6, 1279–1289. https://doi.org/10.1038/s41559-022-01827-7
- Mollel, G.R., Mulungu, D.M.M., Nobert, J., Alexander, A.C., 2023. Assessment of climate change impacts on hydrological processes in the Usangu catchment of Tanzania under CMIP6 scenarios. J. Water Clim. Chang. 14, 4162–4182. https://doi.org/10.2166/wcc.2023.542
- Moomaw, W.R., Chmura, G.L., Davies, G.T., Finlayson, C.M., Middleton, B.A., Natali, S.M., Perry, J.E., Roulet, N., Sutton-Grier, A.E., 2018. Wetlands In a Changing Climate: Science, Policy and Management. Wetlands 38, 183–205. https://doi.org/10.1007/s13157-018-1023-8
- Myhre, G., Alterskjær, K., Stjern, C.W., Hodnebrog, Ø., Marelle, L., Samset, B.H., Sillmann, J., Schaller, N., Fischer, E., Schulz, M., Stohl, A., 2019. Frequency of extreme precipitation increases extensively with event rareness under global warming. Sci. Rep. 9, 16063. https://doi.org/10.1038/s41598-019-52277-4
- Ndehedehe, C., 2023. Hydro-Climatic Extremes: Climate Change and Human Influence, in: Hydro-Climatic Extremes in the Anthropocene. Springer

International Publishing, Cham, pp. 25–55. https://doi.org/10.1007/978-3-031-37727-3_2
- Nitzbon, J., Westermann, S., Langer, M., Martin, L.C.P., Strauss, J., Laboor, S., Boike, J., 2020. Fast response of cold ice-rich permafrost in northeast Siberia to a warming climate. Nat. Commun. 11, 2201. https://doi.org/10.1038/s41467-020-15725-8
- Nyberg, M., Black, T.A., Ketler, R., Lee, S.-C., Johnson, M., Merkens, M., Nugent, K.A., Knox, S.H., 2022. Impacts of Active Versus Passive Re-Wetting on the Carbon Balance of a Previously Drained Bog. J. Geophys. Res. Biogeosciences 127, e2022JG006881. https://doi.org/https://doi.org/10.1029/2022JG006881
- O'Neill, B.C., Tebaldi, C., van Vuuren, D.P., Eyring, V., Friedlingstein, P., Hurtt, G., Knutti, R., Kriegler, E., Lamarque, J.-F., Lowe, J., Meehl, G.A., Moss, R., Riahi, K., Sanderson, B.M., 2016. The Scenario Model Intercomparison Project (ScenarioMIP) for CMIP6. Geosci. Model Dev. 9, 3461–3482. https://doi.org/10.5194/gmd-9-3461-2016
- Ogolo, E.O., Matthew, O.J., 2022. Spatial and temporal analysis of observed trends in extreme precipitation events in different climatic zones of Nigeria. Theor. Appl. Climatol. 148, 1335–1351. https://doi.org/10.1007/s00704-022-04006-7
- Orimoloye, I.R., Kalumba, A.M., Mazinyo, S.P., Nel, W., 2020. Geospatial analysis of wetland dynamics: Wetland depletion and biodiversity conservation of Isimangaliso Wetland, South Africa. J. King Saud Univ. - Sci. 32, 90–96. https://doi.org/10.1016/j.jksus.2018.03.004
- Palmer, P.I., Wainwright, C.M., Dong, B., Maidment, R.I., Wheeler, K.G., Gedney, N., Hickman, J.E., Madani, N., Folwell, S.S., Abdo, G., Allan, R.P., Black, E.C.L., Feng, L., Gudoshava, M., Haines, K., Huntingford, C., Kilavi, M., Lunt, M.F., Shaaban, A., Turner, A.G., 2023. Drivers and impacts of Eastern African rainfall variability. Nat. Rev. Earth Environ. 4, 254–270. https://doi.org/10.1038/s43017-023-00397-x
- Pang, T., Jiang, J., Alfonso, L., Yang, R., Zheng, Y., Wang, P., Zheng, T., 2023. Deriving analytical expressions of the spatial information entropy index on riverine water quality dynamics. J. Hydrol. 623, 129806. https://doi.org/https://doi.org/10.1016/j.jhydrol.2023.129806
- Parkinson, R.W., Wdowinski, S., 2022. Accelerating sea-level rise and the fate of mangrove plant communities in South Florida, U.S.A. Geomorphology 412, 108329. https://doi.org/https://doi.org/10.1016/j.geomorph.2022.108329
- Pendergrass, A.G., Knutti, R., Lehner, F., Deser, C., Sanderson, B.M., 2017. Precipitation variability increases in a warmer climate. Sci. Rep. 7, 17966. https://doi.org/10.1038/s41598-017-17966-y
- Peters-Lidard, C.D., Rose, K.C., Kiang, J.E., Strobel, M.L., Anderson, M.L., Byrd, A.R., Kolian, M.J., Brekke, L.D., Arndt, D.S., 2021. Indicators of climate change impacts on the water cycle and water management. Clim. Change 165, 36. https://doi.org/10.1007/s10584-021-03057-5
- Popoff, N., Gaget, E., Béchet, A., Dami, L., du Rau, P.D., Geijzendorffer, I., Guelmami, A., Mondain-Monval, J.-Y., Perennou, C., Suet, M., Verniest, F., Deschamps, C., Taylor, N.G., Azafzaf, H., Bendjedda, N., Bino, T., Borg, J.J., Božič, L., Dakki, M., Encarnação, V., Erciyas-Yavuz, K., Etayeb, K., Gaudard, C., Hatzofe, O., Langendoen, T., Ieronymidou, C., Mikuska, T., Molina, B., Petkov, N., Portolou, D., Qaneer, T., Sayoud, S., Šćiban, M., Topić, G., Uzunova, D., Vine, G., Vizi, A., Zenatello, M., Abdou, W., Galewski, T., 2021. Gap analysis of the

Ramsar site network at 50: over 150 important Mediterranean sites for wintering waterbirds omitted. Biodivers. Conserv. 30, 3067–3085. https://doi.org/10.1007/s10531-021-02236-1
- Qin, X., Dai, C., Liu, L., 2023. Analyzing future rainfall variations over southern malay peninsula based on CORDEX-SEA dataset. Theor. Appl. Climatol. 152, 407–419. https://doi.org/10.1007/s00704-023-04422-3
- Rakkasagi, S., Goyal, M.K., 2025. Protecting wetlands for future generations: A comprehensive approach to the water-climate-society nexus in South Asia. Environ. Impact Assess. Rev. 115, 107988. https://doi.org/10.1016/j.eiar.2025.107988
- Rakkasagi, S., Goyal, M.K., Jha, S., 2024. Evaluating the future risk of coastal Ramsar wetlands in India to extreme rainfalls using fuzzy logic. J. Hydrol. 632, 130869. https://doi.org/10.1016/j.jhydrol.2024.130869
- Ramsar Convention, 1971. Convention on Wetlands of International Importance especially as Waterfowl Habitat 1–16.
- Ramsar Convention Secretariat, Gardner, C., Finlayson, C.M., Davidson, N., Fennessy, S., Coates, D., van Damm, A., Baker, C., Kumar, R., Stroud, D., Gardner, R.C., Finlayson, C.M., 2018. Global Wetland Outlook: State of the World's Wetlands and their Services to People. Ramsar Conv. Wetl. (2018). 88.
- Regueira, A. de O., Wanderley, H.S., 2022. Changes in rainfall rates and increased number of extreme rainfall events in Rio de Janeiro city. Nat. Hazards 114, 3833–3847. https://doi.org/10.1007/s11069-022-05545-y
- Reid, W., Mooney, H., Cropper, A., Capistrano, D., Carpenter, S., Chopra, K., 2005. Millennium Ecosystem Assessment. Ecosystems and human well-being: synthesis.
- Riahi, K., van Vuuren, D.P., Kriegler, E., Edmonds, J., O'Neill, B.C., Fujimori, S., Bauer, N., Calvin, K., Dellink, R., Fricko, O., Lutz, W., Popp, A., Cuaresma, J.C., KC, S., Leimbach, M., Jiang, L., Kram, T., Rao, S., Emmerling, J., Ebi, K., Hasegawa, T., Havlik, P., Humpenöder, F., Da Silva, L.A., Smith, S., Stehfest, E., Bosetti, V., Eom, J., Gernaat, D., Masui, T., Rogelj, J., Strefler, J., Drouet, L., Krey, V., Luderer, G., Harmsen, M., Takahashi, K., Baumstark, L., Doelman, J.C., Kainuma, M., Klimont, Z., Marangoni, G., Lotze-Campen, H., Obersteiner, M., Tabeau, A., Tavoni, M., 2017. The Shared Socioeconomic Pathways and their energy, land use, and greenhouse gas emissions implications: An overview. Glob. Environ. Chang. 42, 153–168. https://doi.org/https://doi.org/10.1016/j.gloenvcha.2016.05.009
- Rogers, R., Mccann, K., Hoff, R., 1996. Corresponding author address: Quantifying Eff. Humidity Aerosol Scatt. With a Raman Lidar 1–10.
- Rolim, L.Z.R., Oliveira da Silva, S.M., de Souza Filho, F. de A., 2022. Analysis of precipitation dynamics at different timescales based on entropy theory: an application to the State of Ceará, Brazil. Stoch. Environ. Res. Risk Assess. 36, 2285–2301. https://doi.org/10.1007/s00477-021-02112-y
- Roushangar, K., Alizadeh, F., Adamowski, J., Saghebian, S.M., 2019. Exploring the multiscale changeability of precipitation using the entropy concept and self-organizing maps. J. Water Clim. Chang. 11, 655–676. https://doi.org/10.2166/wcc.2019.097
- Sandi, S.G., Rodriguez, J.F., Saintilan, N., Wen, L., Kuczera, G., Riccardi, G., Saco, P.M., 2020. Resilience to drought of dryland wetlands threatened by climate change. Sci. Rep. 10, 13232. https://doi.org/10.1038/s41598-020-70087-x
- Sarkar, S., Maity, R., 2022. Future Characteristics of Extreme Precipitation Indicate the Dominance of Frequency Over Intensity: A Multi-Model Assessment From

CMIP6 Across India. J. Geophys. Res. Atmos. 127, e2021JD035539. https://doi.org/https://doi.org/10.1029/2021JD035539
- Sarkar, S., Maity, R., 2021. Global climate shift in 1970s causes a significant worldwide increase in precipitation extremes. Sci. Rep. 11, 11574. https://doi.org/10.1038/s41598-021-90854-8
- Schrapffer, A., Sörensson, A., Polcher, J., Fita, L., 2020. Benefits of representing floodplains in a Land Surface Model: Pantanal simulated with ORCHIDEE CMIP6 version. Clim. Dyn. 55, 1303–1323. https://doi.org/10.1007/s00382-020-05324-0
- Schuerch, M., Spencer, T., Temmerman, S., Kirwan, M.L., Wolff, C., Lincke, D., McOwen, C.J., Pickering, M.D., Reef, R., Vafeidis, A.T., Hinkel, J., Nicholls, R.J., Brown, S., 2018. Future response of global coastal wetlands to sea-level rise. Nature 561, 231–234. https://doi.org/10.1038/s41586-018-0476-5
- Schuur, E.A.G., McGuire, A.D., Schädel, C., Grosse, G., Harden, J.W., Hayes, D.J., Hugelius, G., Koven, C.D., Kuhry, P., Lawrence, D.M., Natali, S.M., Olefeldt, D., Romanovsky, V.E., Schaefer, K., Turetsky, M.R., Treat, C.C., Vonk, J.E., 2015. Climate change and the permafrost carbon feedback. Nature 520, 171–179. https://doi.org/10.1038/nature14338
- Sebaziga, N.J., Safari, B., Ngaina, J.N., Ntwali, D., 2025. Observed trends and variability of seasonal extreme rainfall indices and projected changes in Rwanda. Theor. Appl. Climatol. 156, 245. https://doi.org/10.1007/s00704-025-05474-3
- Seneviratne, S.I., Nicholls, N., Easterling, D., Goodess, C.M., Kanae, S., Kossin, J., Luo, Y., Marengo, J., Mc Innes, K., Rahimi, M., Reichstein, M., Sorteberg, A., Vera, C., Zhang, X., Rusticucci, M., Semenov, V., Alexander, L. V., Allen, S., Benito, G., Cavazos, T., Clague, J., Conway, D., Della-Marta, P.M., Gerber, M., Gong, S., Goswami, B.N., Hemer, M., Huggel, C., Van den Hurk, B., Kharin, V. V., Kitoh, A., Klein Tank, A.M.G., Li, G., Mason, S., Mc Guire, W., Van Oldenborgh, G.J., Orlowsky, B., Smith, S., Thiaw, W., Velegrakis, A., Yiou, P., Zhang, T., Zhou, T., Zwiers, F.W., 2012. Changes in climate extremes and their impacts on the natural physical environment. Manag. Risks Extrem. Events Disasters to Adv. Clim. Chang. Adapt. Spec. Rep. Intergov. Panel Clim. Chang. 9781107025, 109–230. https://doi.org/10.1017/CBO9781139177245.006
- Shannon, C.E., 1948. A Mathematical Theory of Communication. Bell Syst. Tech. J. 27, 379–423. https://doi.org/10.1002/j.1538-7305.1948.tb01338.x
- Sharma, L.K., Naik, R., 2024. Wetland Ecosystems, in: Conservation of Saline Wetland Ecosystems: An Initiative towards UN Decade of Ecological Restoration. Springer Nature Singapore, Singapore, pp. 3–32. https://doi.org/10.1007/978-981-97-5069-6_1
- Sharma, S., Phartiyal, M., Madhav, S., Singh, P., 2021. Global Wetlands, in: Wetlands Conservation. Wiley, pp. 1–16. https://doi.org/10.1002/9781119692621.ch1
- Shuangcheng, L., Qiaofu, Z., Shaohong, W., Erfu, D., 2006. Measurement of climate complexity using sample entropy. Int. J. Climatol. 26, 2131–2139. https://doi.org/10.1002/joc.1357
- Shukla, K., Shukla, S., Upadhyay, D., Singh, V., Mishra, A., Jindal, T., 2021. Socio-Economic Assessment of Climate Change Impact on Biodiversity and Ecosystem Services, in: Choudhary, D.K., Mishra, A., Varma, A. (Eds.), Climate Change and the Microbiome: Sustenance of the Ecosphere. Springer International Publishing, Cham, pp. 661–694. https://doi.org/10.1007/978-3-030-76863-8_34
- Sillmann, J., Kharin, V. V., Zwiers, F.W., Zhang, X., Bronaugh, D., 2013. Climate

extremes indices in the CMIP5 multimodel ensemble: Part 2. Future climate projections. J. Geophys. Res. Atmos. 118, 2473–2493. https://doi.org/10.1002/jgrd.50188
- Simpkins, G., 2017. Progress in climate modelling. Nat. Clim. Chang. 7, 684–685. https://doi.org/10.1038/nclimate3398
- Singh, S., Goyal, M.K., Saikumar, E., 2024. Assessing Climate Vulnerability of Ramsar Wetlands through CMIP6 Projections. Water Resour. Manag. 38, 1381–1395. https://doi.org/10.1007/s11269-023-03726-3
- Singh, S., Kumar, A., 2024. Understanding the intricacies of rainfall dynamics using entropy measures. J. Water Clim. Chang. 15, 4817–4839. https://doi.org/10.2166/wcc.2024.350
- Singh, S., Kumar, D., Kumar, A., 2022. Entropy based assessment of rainfall dynamics with varying elevations for hilly areas of Uttarakhand, India. https://doi.org/10.21203/rs.3.rs-2204882/v1
- Singh, S., Kumar, N., Goyal, M.K., Jha, S., 2023. Relative influence of ENSO, IOD, and AMO over spatiotemporal variability of hydroclimatic extremes in Narmada basin, India. AQUA — Water Infrastructure, Ecosyst. Soc. 72, 520–539. https://doi.org/10.2166/aqua.2023.219
- Singh, V.P., 2013. Entropy Theory and its Application in Environmental and Water Engineering. Wiley. https://doi.org/10.1002/9781118428306
- Singh, V.P., 2011. Hydrologic Synthesis Using Entropy Theory: Review. J. Hydrol. Eng. 16, 421–433. https://doi.org/10.1061/ (ASCE)HE.1943-5584.0000332
- Singh, V.P., 1997. THE USE OF ENTROPY IN HYDROLOGY AND WATER RESOURCES. Hydrol. Process. 11, 587–626. https://doi.org/10.1002/ (SICI)1099-1085 (199705)11:6<587::AID-HYP479>3.0.CO;2-P
- Skea, J., Shukla, P., Al Khourdajie, A., McCollum, D., 2021. Intergovernmental Panel on Climate Change: Transparency and integrated assessment modeling. WIREs Clim. Chang. 12, e727. https://doi.org/https://doi.org/10.1002/wcc.727
- Skliris, N., Marsh, R., Haigh, I.D., Wood, M., Hirschi, J., Darby, S., Quynh, N.P., Hung, N.N., 2022. Drivers of rainfall trends in and around Mainland Southeast Asia. Front. Clim. Volume 4-. https://doi.org/10.3389/fclim.2022.926568
- Spencer, T., Schuerch, M., Nicholls, R.J., Hinkel, J., Lincke, D., Vafeidis, A.T., Reef, R., McFadden, L., Brown, S., 2016. Global coastal wetland change under sea-level rise and related stresses: The DIVA Wetland Change Model. Glob. Planet. Change 139, 15–30. https://doi.org/https://doi.org/10.1016/j.gloplacha.2015.12.018
- Sreeparvathy, V., Srinivas, V. V, 2022. Global assessment of spatiotemporal variability of wet, normal and dry conditions using multiscale entropy-based approach. Sci. Rep. 12, 9767. https://doi.org/10.1038/s41598-022-13830-w
- Swain, S., Mishra, S.K., Pandey, A., Dayal, D., 2022. Spatiotemporal assessment of precipitation variability, seasonality, and extreme characteristics over a Himalayan catchment. Theor. Appl. Climatol. 147, 817–833. https://doi.org/10.1007/s00704-021-03861-0
- Tabari, H., 2020. Climate change impact on flood and extreme precipitation increases with water availability. Sci. Rep. 10, 13768. https://doi.org/10.1038/s41598-020-70816-2
- Tatli, H., Dalfes, H.N., 2021. Analysis of temporal diversity of precipitation along with biodiversity of Holdridge life zones. Theor. Appl. Climatol. 144, 391–400. https://doi.org/10.1007/s00704-021-03551-x

- Teuchies, J., Vandenbruwaene, W., Carpentier, R., Bervoets, L., Temmerman, S., Wang, C., Maris, T., Cox, T.J.S., Van Braeckel, A., Meire, P., 2013. Estuaries as Filters: The Role of Tidal Marshes in Trace Metal Removal. PLoS One 8, 1–11. https://doi.org/10.1371/journal.pone.0070381
- Thrasher, B., Maurer, E.P., McKellar, C., Duffy, P.B., 2012. Technical Note: Bias correcting climate model simulated daily temperature extremes with quantile mapping. Hydrol. Earth Syst. Sci. 16, 3309–3314. https://doi.org/10.5194/hess-16-3309-2012
- Thrasher, B., Wang, W., Michaelis, A., Melton, F., Lee, T., Nemani, R., 2022. NASA Global Daily Downscaled Projections, CMIP6. Sci. Data 9, 262. https://doi.org/10.1038/s41597-022-01393-4
- Thrasher, B., Xiong, J., Wang, W., Melton, F., Michaelis, A., Nemani, R., 2013. Downscaled Climate Projections Suitable for Resource Management. Eos, Trans. Am. Geophys. Union 94, 321–323. https://doi.org/10.1002/2013EO370002
- Tung, Y.-S., Wang, C.-Y., Weng, S.-P., Yang, C.-D., 2022. Extreme index trends of daily gridded rainfall dataset (1960–2017) in Taiwan. Terr. Atmos. Ocean. Sci. 33, 8. https://doi.org/10.1007/s44195-022-00009-z
- Valenti, V.L., Carcelen, E.C., Lange, K., Russo, N.J., Chapman, B., 2020. Leveraging Google Earth Engine User Interface for Semiautomated Wetland Classification in the Great Lakes Basin at 10 m With Optical and Radar Geospatial Datasets. IEEE J. Sel. Top. Appl. Earth Obs. Remote Sens. 13, 6008–6018. https://doi.org/10.1109/JSTARS.2020.3023901
- van Vuuren, D.P., Edmonds, J., Kainuma, M., Riahi, K., Thomson, A., Hibbard, K., Hurtt, G.C., Kram, T., Krey, V., Lamarque, J.-F., Masui, T., Meinshausen, M., Nakicenovic, N., Smith, S.J., Rose, S.K., 2011. The representative concentration pathways: an overview. Clim. Change 109, 5–31. https://doi.org/10.1007/s10584-011-0148-z
- Wang, H., Liu, J., Klaar, M., Chen, A., Gudmundsson, L., Holden, J., 2024. Anthropogenic climate change has influenced global river flow seasonality. Science (80-.). 383, 1009–1014. https://doi.org/10.1126/science.adi9501
- Wang, L., Wang, J., He, F., Wang, Q., Zhao, Y., Lu, P., Huang, Y., Cui, H., Deng, H., Jia, X., 2023. Spatial–temporal variation of extreme precipitation in the Yellow–Huai–Hai–Yangtze Basin of China. Sci. Rep. 13, 9312. https://doi.org/10.1038/s41598-023-36470-0
- Wang, P., Huang, Q., Tang, Q., Chen, X., Yu, J., Pozdniakov, S.P., Wang, T., 2021. Increasing annual and extreme precipitation in permafrost-dominated Siberia during 1959–2018. J. Hydrol. 603, 126865. https://doi.org/https://doi.org/10.1016/j.jhydrol.2021.126865
- Wang, R., Ding, J., Ge, X., Wang, J., Qin, S., Tan, J., Han, L., Zhang, Z., 2023. Impacts of climate change on the wetlands in the arid region of Northwestern China over the past 2 decades. Ecol. Indic. 149, 110168. https://doi.org/https://doi.org/10.1016/j.ecolind.2023.110168
- Wang, X.-L., Feng, A.-Q., Hou, X.-Y., Chao, Q.-C., Song, B.-Y., Liu, Y.-B., Wang, Q.-G., Xu, H., Zhang, Y.-X., Li, D., Dong, L.-J., Guo, Y., 2024. Compound extreme inundation risk of coastal wetlands caused by climate change and anthropogenic activities in the Yellow River Delta, China. Adv. Clim. Chang. Res. 15, 134–147. https://doi.org/https://doi.org/10.1016/j.accre.2024.01.010
- Wehner, M., Lee, J., Risser, M., Ullrich, P., Gleckler, P., Collins, W.D., 2021. Evaluation of extreme sub-daily precipitation in high-resolution global climate

model simulations. Philos. Trans. R. Soc. A Math. Phys. Eng. Sci. 379, 20190545. https://doi.org/10.1098/rsta.2019.0545

- Were, D., Kansiime, F., Fetahi, T., Cooper, A., Jjuuko, C., 2019. Carbon Sequestration by Wetlands: A Critical Review of Enhancement Measures for Climate Change Mitigation. Earth Syst. Environ. 3, 327–340. https://doi.org/10.1007/s41748-019-00094-0
- Wilson, A.B., Avila-Diaz, A., Oliveira, L.F., Zuluaga, C.F., Mark, B., 2022. Climate extremes and their impacts on agriculture across the Eastern Corn Belt Region of the U.S. Weather Clim. Extrem. 37, 100467. https://doi.org/10.1016/j.wace.2022.100467
- Wood, A.W., Leung, L.R., Sridhar, V., Lettenmaier, D.P., 2004. Hydrologic Implications of Dynamical and Statistical Approaches to Downscaling Climate Model Outputs. Clim. Change 62, 189–216. https://doi.org/10.1023/B:CLIM.0000013685.99609.9e
- Wu, Y., Sun, J., Hu, B., Xu, Y.J., Rousseau, A.N., Zhang, G., 2023. Can the combining of wetlands with reservoir operation reduce the risk of future floods and droughts? Hydrol. Earth Syst. Sci. 27, 2725–2745. https://doi.org/10.5194/hess-27-2725-2023
- Wu, Y., Sun, J., Jun Xu, Y., Zhang, G., Liu, T., 2022. Projection of future hydrometeorological extremes and wetland flood mitigation services with different global warming levels: A case study in the Nenjiang river basin. Ecol. Indic. 140, 108987. https://doi.org/10.1016/j.ecolind.2022.108987
- Wu, Y., Yin, X., Zhou, G., Bruijnzeel, L.A., Dai, A., Wang, F., Gentine, P., Zhang, G., Song, Y., Zhou, D., 2024. Rising rainfall intensity induces spatially divergent hydrological changes within a large river basin. Nat. Commun. 15, 823. https://doi.org/10.1038/s41467-023-44562-8
- Xi, Y., Peng, S., Ciais, P., Chen, Y., 2021. Future impacts of climate change on inland Ramsar wetlands. Nat. Clim. Chang. 11, 45–51. https://doi.org/10.1038/s41558-020-00942-2
- Xiong, Y., Mo, S., Wu, H., Qu, X., Liu, Y., Zhou, L., 2023. Influence of human activities and climate change on wetland landscape pattern—A review. Sci. Total Environ. 879, 163112. https://doi.org/https://doi.org/10.1016/j.scitotenv.2023.163112
- Xu, D., Bisht, G., Tan, Z., Sinha, E., Di Vittorio, A. V, Zhou, T., Ivanov, V.Y., Leung, L.R., 2024. Climate change will reduce North American inland wetland areas and disrupt their seasonal regimes. Nat. Commun. 15, 2438. https://doi.org/10.1038/s41467-024-45286-z
- Yaduvanshi, A., Sinha, A.K., Haldar, K., 2019. A century scale hydro-climatic variability and associated risk in Subarnarekha river basin of India. Model. Earth Syst. Environ. 5, 937–949. https://doi.org/10.1007/s40808-019-00580-4
- Yan, W., Wang, Y., Chaudhary, P., Ju, P., Zhu, Q., Kang, X., Chen, H., He, Y., 2022. Effects of climate change and human activities on net primary production of wetlands on the Zoige Plateau from 1990 to 2015. Glob. Ecol. Conserv. 35, e02052. https://doi.org/https://doi.org/10.1016/j.gecco.2022.e02052
- Yao, J., Chen, Y., Chen, J., Zhao, Y., Tuoliewubieke, D., Li, J., Yang, L., Mao, W., 2021. Intensification of extreme precipitation in arid Central Asia. J. Hydrol. 598, 125760. https://doi.org/https://doi.org/10.1016/j.jhydrol.2020.125760
- Yeşilırmak, E., Atatanır, L., 2016. Spatiotemporal variability of precipitation concentration in western Turkey. Nat. Hazards 81, 687–704.

https://doi.org/10.1007/s11069-015-2102-2
- Yin, H., Sun, Y., 2018. Characteristics of extreme temperature and precipitation in China in 2017 based on ETCCDI indices. Adv. Clim. Chang. Res. 9, 218–226. https://doi.org/10.1016/j.accre.2019.01.001
- Yin, J., Guo, S., Wang, J., Chen, J., Zhang, Q., Gu, L., Yang, Y., Tian, J., Xiong, L., Zhang, Y., 2023. Thermodynamic driving mechanisms for the formation of global precipitation extremes and ecohydrological effects. Sci. China Earth Sci. 66, 92–110. https://doi.org/10.1007/s11430-022-9987-0
- Yu, Y., Schneider, U., Yang, S., Becker, A., Ren, Z., 2020. Evaluating the GPCC Full Data Daily Analysis Version 2018 through ETCCDI indices and comparison with station observations over mainland of China. Theor. Appl. Climatol. 142, 835–845. https://doi.org/10.1007/s00704-020-03352-8
- Zhang, C., Zhou, X., Lei, W., 2019. Necessary length of daily precipitation time series for different entropy measures. Earth Sci. Informatics 12. https://doi.org/10.1007/s12145-019-00392-1
- Zhang, L., Li, H., Liu, D., Fu, Q., Li, M., Faiz, M.A., Khan, M.I., Li, T., 2019. Identification and application of the most suitable entropy model for precipitation complexity measurement. Atmos. Res. 221, 88–97. https://doi.org/https://doi.org/10.1016/j.atmosres.2019.02.002
- Zhang, M., Yuan, N., Lin, H., Liu, Y., Zhang, H., 2022. Quantitative estimation of the factors impacting spatiotemporal variation in NPP in the Dongting Lake wetlands using Landsat time series data for the last two decades. Ecol. Indic. 135, 108544. https://doi.org/https://doi.org/10.1016/j.ecolind.2022.108544
- Zhang, W., Furtado, K., Wu, P., Zhou, T., Chadwick, R., Marzin, C., Rostron, J., Sexton, D., 2021. Increasing precipitation variability on daily-to-multiyear time scales in a warmer world. Sci. Adv. 7, eabf8021. https://doi.org/10.1126/sciadv.abf8021
- Zhang, X., Alexander, L., Hegerl, G.C., Jones, P., Tank, A.K., Peterson, T.C., Trewin, B., Zwiers, F.W., 2011. Indices for monitoring changes in extremes based on daily temperature and precipitation data. WIREs Clim. Chang. 2, 851–870. https://doi.org/10.1002/wcc.147
- Zhang, Y., Li, W., Sun, G., King, J., 2022. Coastal Wetland Hydrologic Resilience to Climatic Disturbances: Concept, Quantification, and Threshold Response, in: Eslamian, S., Eslamian, F. (Eds.), Disaster Risk Reduction for Resilience: Disaster and Social Aspects. Springer International Publishing, Cham, pp. 417–429. https://doi.org/10.1007/978-3-030-99063-3_18
- Zhao, M., Boll, J., 2022. Adaptation of water resources management under climate change. Front. Water Volume 4-. https://doi.org/10.3389/frwa.2022.983228
- Zheng, K., Tan, L., Sun, Y., Wu, Y., Duan, Z., Xu, Y., Gao, C., 2021. Impacts of climate change and anthropogenic activities on vegetation change: Evidence from typical areas in China. Ecol. Indic. 126, 107648. https://doi.org/https://doi.org/10.1016/j.ecolind.2021.107648
- Zittis, G., Bruggeman, A., Lelieveld, J., 2021. Revisiting future extreme precipitation trends in the Mediterranean. Weather Clim. Extrem. 34, 100380. https://doi.org/https://doi.org/10.1016/j.wace.2021.100380
- Zou, S., Abuduwaili, J., Duan, W., Ding, J., De Maeyer, P., Van De Voorde, T., Ma, L., 2021. Attribution of changes in the trend and temporal non-uniformity of extreme precipitation events in Central Asia. Sci. Rep. 11, 15032. https://doi.org/10.1038/s41598-021-94486-w